

## Quantum asymptotic amplitude for quantum oscillatory systems from the Koopman operator viewpoint

Yuzuru Kato<sup>1, a)</sup>

*Department of Complex and Intelligent Systems, Future University Hakodate,  
Hokkaido 041-8655, Japan*

(Dated: 29 March 2024)

We have recently proposed a fully quantum-mechanical definition of the asymptotic phase for quantum nonlinear oscillators, which is also applicable in the strong quantum regime [Kato and Nakao 2022 Chaos 32 063133]. In this study, we propose a definition of the quantum asymptotic amplitude for quantum oscillatory systems, which extends naturally the definition of the asymptotic amplitude for classical nonlinear oscillators on the basis of the Koopman operator theory. We introduce the asymptotic amplitude for quantum oscillatory systems by using the eigenoperator of the backward Liouville operator associated with the largest non-zero real eigenvalue. Using examples of the quantum van der Pol oscillator with the quantum Kerr effect, exhibiting quantum limit-cycle oscillations, and the quantum van der Pol model with the quantum squeezing and degenerate parametric oscillator with nonlinear damping, exhibiting quantum noise-induced oscillations, we illustrate that the proposed quantum asymptotic amplitude appropriately yields isostable amplitude values that decay exponentially with a constant rate.

---

<sup>a)</sup>Electronic mail: Corresponding author: [katoyuzu@fun.ac.jp](mailto:katoyuzu@fun.ac.jp)

Rhythmic oscillations and synchronization are widely observed in various fields of science and technology. Recent advances in nanotechnology facilitate the analysis of quantum rhythmic oscillations and synchronization. The asymptotic phase and amplitude functions are fundamental quantities of classical nonlinear oscillators and have been used for the systematic analysis and control of synchronization phenomena. We have recently introduced a fully quantum mechanical definition of the asymptotic phase for quantum oscillatory systems, while the quantum asymptotic amplitude has remained unexplored. In this study, we propose a fully quantum mechanical definition of the asymptotic amplitude for quantum oscillatory systems, which extends naturally the definition of the asymptotic amplitude for classical oscillatory systems on the basis of the Koopman operator theory. The proposed quantum asymptotic amplitude appropriately yields isostable amplitude values in examples of systems exhibiting quantum limit-cycle oscillations and quantum noise-induced oscillations.

## I. INTRODUCTION

Synchronization phenomena are ubiquitously observed in nature. Since Huygens first documented the discovery of mutual synchronization between two pendulum clocks, synchronization of classical oscillatory systems has been extensively studied in various fields of science and technology, such as flashing fireflies, chorusing crickets, circadian clocks, chemical oscillations, and electrical oscillators<sup>1-6</sup>. Owing to recent advances in nanotechnology, experimental observations of quantum phase synchronization have been reported in spin-1 atoms<sup>7</sup>, nuclear spin systems<sup>8</sup>, and on the IBM Q system<sup>9</sup>, along with extensive theoretical studies on quantum synchronization<sup>10-37</sup>

Rhythmic oscillations in classical deterministic systems can be modeled as nonlinear dynamical systems possessing stable limit-cycle solutions. The *asymptotic phase* and *isochron*<sup>1-5</sup>, which increase linearly with a constant frequency in the basin of the limit cycle, are fundamental quantities for the analysis of synchronization phenomena. Recent findings have pointed out that the asymptotic phase, originally proposed by Winfree<sup>38</sup> and Guckenheimer<sup>39</sup> from a geometrical viewpoint<sup>38,39</sup>, has an intimate relationship with the Koopman eigenfunction associated with the fundamental frequency of the oscillator<sup>40-45</sup>.

Moreover, the *asymptotic amplitudes* and *isostables*, which characterize deviation from the limit cycle and exhibit exponential decay with constant rates to the limit cycle, have been naturally introduced in terms of the Koopman eigenfunction associated with the Floquet exponents with non-zero real parts<sup>40–46</sup>. These phase and amplitude functions are fundamental quantities for characterizing limit-cycle oscillations, and the resulting phase-amplitude reduction<sup>40–45,47,48</sup> provides a useful framework for the analysis and control of synchronization dynamics.

The phase and amplitude description can also be extended to classical stochastic oscillatory systems. The stochastic asymptotic phase<sup>49</sup>, which increases with a constant frequency on average with the stochastic evolution of the system, has been introduced in terms of the slowest decaying eigenfunction of the backward Fokker-Planck (Kolmogorov) operator describing the mean first passage time. Similarly, the stochastic asymptotic amplitude<sup>50</sup>, which decays exponentially with a constant rate on average with the stochastic evolution of the system, has been introduced in terms of the eigenfunction associated with the largest non-zero real eigenvalue. These definitions of stochastic asymptotic phase and amplitude have relationships with stochastic Koopman operator theory<sup>51–53</sup> and can be regarded as a natural extension of the deterministic definitions from the Koopman operator viewpoint<sup>54</sup>.

By extending the definition of the stochastic asymptotic phase from the Koopman operator viewpoint, we have recently introduced a fully quantum-mechanical definition of the asymptotic phase for quantum oscillatory systems, which increases linearly with the evolution of the quantum state and provides appropriate phase values for characterizing quantum synchronization even in the strong quantum regime<sup>35,36</sup>. On the other hand, the quantum asymptotic amplitude functions for quantum oscillatory systems have remained unexplored.

In this study, we propose a fully quantum-mechanical definition of the asymptotic amplitude for quantum oscillatory systems, by extending the definition of the stochastic asymptotic amplitude from the Koopman-operator viewpoint. We define the quantum asymptotic amplitude for quantum oscillatory systems using the eigenoperator of the backward Liouville operator associated with the largest non-zero real eigenvalue. Using examples of the quantum van der Pol oscillator with the quantum Kerr effect, exhibiting quantum limit-cycle oscillations, and the quantum van der Pol model with the quantum squeezing and degenerate parametric oscillator with nonlinear damping, exhibiting quantum noise-induced oscillations, we numerically demonstrate that the proposed quantum asymptotic amplitude

yields appropriate amplitude values that decay exponentially with a constant rate with the evolution of the quantum state.

## II. ASYMPTOTIC PHASE AND AMPLITUDE FOR CLASSICAL OSCILLATORY SYSTEMS

### A. Deterministic oscillatory systems

Firstly, we provide a brief overview of the asymptotic phase and amplitude for deterministic limit-cycle oscillators and discuss their relationship with the Koopman operator theory<sup>40–43,45</sup>.

We consider a deterministic dynamical system

$$\dot{\mathbf{X}}(t) = \mathbf{A}(\mathbf{X}(t)), \quad (1)$$

where  $\mathbf{X}(t) \in \mathbb{R}^N$  represents the system state at time  $t$ ,  $\mathbf{A}(\mathbf{X}) \in \mathbb{R}^N$  is a sufficiently smooth vector field governing the system dynamics, and  $(\dot{\phantom{x}})$  denotes the time derivative.

We assume that the system possesses an exponentially stable limit-cycle solution  $\mathbf{X}_0(t)$  with a natural period  $T$  and frequency  $\Omega_c = 2\pi/T$ , satisfying  $\mathbf{X}_0(t+T) = \mathbf{X}_0(t)$ . We let  $\chi_c$  and  $B_\chi \subseteq \mathbb{R}^N$  denote the limit cycle and its basin of attraction, respectively. Instead of using the time  $t$ , we parameterize a point on the limit cycle  $\chi$  by a phase  $\phi \in [0, 2\pi)$  as  $\chi(\phi) = \mathbf{X}_0(\Omega_c t)$  ( $0 \leq t < T$ ), where the phase value  $\phi = \Omega_c t$  increases linearly with time  $t$  from 0 to  $2\pi$  ( $2\pi$  is identified with 0). We can set the origin of the phase  $\phi = 0$  to the state  $\mathbf{X}_0(0)$  without loss of generality.

The linear stability of the limit cycle is characterized by the Floquet exponents  $\Lambda_j \in \mathbb{C}$  ( $j = 0, 1, \dots, N-1$ )<sup>55</sup> and can be arranged in decreasing order of their real parts as  $\text{Re}(\Lambda_0) \geq \text{Re}(\Lambda_1) \geq \text{Re}(\Lambda_2) \geq \dots \geq \text{Re}(\Lambda_{N-1})$ . The exponent  $\Lambda_0$  is zero and associated with the phase direction tangent to  $\chi_c$ . The other exponents  $\Lambda_1, \dots, \Lambda_{N-1}$  are associated with the amplitude directions departing from  $\chi_c$  and possess negative real parts due to the exponential stability of  $\chi_c$ . Additionally, we assume that  $\kappa_c = \Lambda_1$  is real and much larger than  $\text{Re}(\Lambda_2)$ , indicating that the relaxation of the slowest decaying mode is non-oscillatory and much slower than the other faster decaying modes. We can then focus only on the slowest decaying mode and introduce a single real amplitude associated with it. Such a situation is natural in realistic models of limit cycle oscillators.

The asymptotic phase function  $\Phi_c : B_\chi \rightarrow [0, 2\pi)$  and amplitude function  $R_c : B_\chi \rightarrow \mathbb{R}$  can be introduced in the basin  $B_\chi$  of  $\chi_c$ , which satisfy<sup>43</sup>

$$\begin{aligned}\mathbf{A}(\mathbf{X}) \cdot \nabla \Phi_c(\mathbf{X}) &= \Omega_c, \\ \mathbf{A}(\mathbf{X}) \cdot \nabla R_c(\mathbf{X}) &= \kappa_c R_c(\mathbf{X}),\end{aligned}\tag{2}$$

with the inner product defined as  $\mathbf{a} \cdot \mathbf{b} = \sum_{j=1}^N \overline{a_j} b_j$  (the overline denotes complex conjugate) and  $\nabla = \partial/\partial \mathbf{X}$  representing the gradient with respect to  $\mathbf{X}$ . Specifically, we focus only on the phase associated with  $\Lambda_0 = 0$  and the slowest decaying amplitude associated with the real eigenvalue  $\Lambda_1 (= \kappa_c)$ . In general, we can introduce  $N - 1$  amplitude variables associated with  $N - 1$  exponents  $\Lambda_1, \dots, \Lambda_{N-1}$ , which are generally complex, and derive a closed set of phase-amplitude equations for the phase and amplitudes characterizing the convergence to the limit-cycle attractors in details<sup>43</sup>. The level sets of the phase function are referred to as *isochrons*<sup>38,39</sup>, and those of the amplitude function as *isostables*<sup>40</sup>.

From these functions, we can introduce the phase and amplitude variables for the oscillator state  $\mathbf{X}(t) \in B_\chi$  at time  $t$  as  $\phi(t) = \Phi_c(\mathbf{X}(t))$  and  $r(t) = R_c(\mathbf{X}(t))$ , satisfying

$$\begin{aligned}\dot{\phi}(t) &= \dot{\Phi}_c(\mathbf{X}(t)) = \mathbf{A}(\mathbf{X}(t)) \cdot \nabla \Phi_c(\mathbf{X}(t)) = \Omega_c, \\ \dot{r}(t) &= \dot{R}_c(\mathbf{X}(t)) = \mathbf{A}(\mathbf{X}(t)) \cdot \nabla R_c(\mathbf{X}(t)) = \kappa_c R_c(\mathbf{X}) = \kappa_c r(t),\end{aligned}\tag{3}$$

where the phase  $\phi$  always increases with a constant frequency  $\Omega_c$ , and the amplitude  $r$  decays exponentially with a rate  $\kappa_c$ , when the state  $\mathbf{X}$  evolves in  $B_\chi$  toward  $\chi_c$ .

The linear operator  $A_c = \mathbf{A}(\mathbf{X}) \cdot \nabla$  in the above definitions of the asymptotic phase and amplitude serves as the infinitesimal generator of the *Koopman operator*, describing the time evolution of observables for the system in Eq. (1) (see Refs.<sup>40-43</sup> for further details).

We can confirm that the complex exponential  $\Psi_c(\mathbf{X}) = e^{i\Phi_c(\mathbf{X})}$  of  $\Phi_c(\mathbf{X})$  is an eigenfunction of  $A_c$  with the eigenvalue  $i\Omega_c$ , expressed as  $A_c \Psi_c(\mathbf{X}) = i\Omega_c \Psi_c(\mathbf{X})$ . Thus, we can introduce the asymptotic phase using the Koopman eigenfunction  $\Psi_c(\mathbf{X})$  of  $A_c$  as

$$\Phi_c(\mathbf{X}) = \arg \Psi_c(\mathbf{X}).\tag{4}$$

Likewise, we can introduce the asymptotic amplitude  $R_c(\mathbf{X})$  using the Koopman eigenfunction of  $A_c$  associated with the eigenvalue  $\kappa_c$  as

$$A_c R_c(\mathbf{X}) = \kappa_c R_c(\mathbf{X}).\tag{5}$$

Hence, the Koopman operator theory offers a natural and unified definition of the asymptotic phase, which increases with a constant frequency, and the amplitude, which decays exponentially with a constant rate. Mauroy and Mezić<sup>40,44,56</sup> have clarified these relationships and provided explicit numerical methods for calculating the phase and amplitude functions for various models of limit-cycle oscillators.

## B. Stochastic oscillatory systems

The asymptotic phase<sup>49</sup> and amplitude<sup>50</sup> can also be introduced for stochastic oscillatory systems on the basis of the Koopman operator theory. In stochastic oscillatory systems, defining the asymptotic phase and amplitude cannot rely on the deterministic limit-cycle attractor unless the noise is sufficiently small.

Consider a stochastic dynamical system described by an Ito stochastic differential equation (SDE)

$$d\mathbf{X}(t) = \mathbf{A}(\mathbf{X}(t))dt + \mathbf{B}(\mathbf{X}(t))d\mathbf{W}(t), \quad (6)$$

where  $\mathbf{X}(t) \in \mathbb{R}^N$  represents the system state at time  $t$ ,  $\mathbf{A}(\mathbf{X}) \in \mathbb{R}^N$  represents a drift vector representing the deterministic dynamics,  $\mathbf{B}(\mathbf{X}) \in \mathbb{R}^{N \times N}$  represents a matrix characterizing the effect of the noise, and  $\mathbf{W}(t) \in \mathbb{R}^N$  is an  $N$ -dimensional Wiener process.

The forward and backward Fokker-Planck equations<sup>57</sup>, corresponding to the SDE (6), describe the time evolution of the transition probability density  $p(\mathbf{X}, t | \mathbf{Y}, s)$  ( $t \geq s$ ) as

$$\frac{\partial}{\partial t} p(\mathbf{X}, t | \mathbf{Y}, s) = L_{\mathbf{X}} p(\mathbf{X}, t | \mathbf{Y}, s), \quad (7)$$

and

$$\frac{\partial}{\partial s} p(\mathbf{X}, t | \mathbf{Y}, s) = -L_{\mathbf{Y}}^* p(\mathbf{X}, t | \mathbf{Y}, s), \quad (8)$$

respectively, where the (forward) Fokker-Planck operator is expressed as

$$L_{\mathbf{X}} = -\frac{\partial}{\partial \mathbf{X}} \mathbf{A}(\mathbf{X}) + \frac{1}{2} \frac{\partial^2}{\partial \mathbf{X}^2} \mathbf{D}(\mathbf{X}), \quad (9)$$

and the backward Fokker-Planck operator is expressed as (in terms of  $\mathbf{X}$ )

$$L_{\mathbf{X}}^* = \mathbf{A}(\mathbf{X}) \frac{\partial}{\partial \mathbf{X}} + \frac{1}{2} \mathbf{D}(\mathbf{X}) \frac{\partial^2}{\partial \mathbf{X}^2}, \quad (10)$$

where  $\mathbf{D}(\mathbf{X}) = \mathbf{B}(\mathbf{X})\mathbf{B}(\mathbf{X})^\top \in \mathbb{R}^{N \times N}$  represents a matrix of diffusion coefficients ( $\top$  indicates the matrix transposition). The forward and backward operators  $L_{\mathbf{X}}$  and  $L_{\mathbf{X}}^*$  are mutually adjoint, i.e.,  $\langle L_{\mathbf{X}}G(\mathbf{X}), H(\mathbf{X}) \rangle_{\mathbf{X}} = \langle G(\mathbf{X}), L_{\mathbf{X}}^*H(\mathbf{X}) \rangle_{\mathbf{X}}$ , where the inner product is defined as  $\langle G(\mathbf{X}), H(\mathbf{X}) \rangle_{\mathbf{X}} = \int \overline{G(\mathbf{X})}H(\mathbf{X})d\mathbf{X}$  for two functions  $G(\mathbf{X}), H(\mathbf{X}) : \mathbb{R}^N \rightarrow \mathbb{C}$ . The integration is taken over the whole range of  $\mathbf{X}$ .

Let  $p(\mathbf{X}) \in \mathbb{R}$  denote the probability density function of  $\mathbf{X}$ , satisfying the Fokker-Planck equation  $\partial p(\mathbf{X})/\partial t = L_{\mathbf{X}}p(\mathbf{X})$ , and  $g : \mathbb{R}^N \rightarrow \mathbb{C}$  denote an observable of the system, which maps the system state  $\mathbf{X}$  to a complex value. The evolution of the expectation  $\langle g \rangle_s = \int p(\mathbf{X})g(\mathbf{X})d\mathbf{X} = \langle p(\mathbf{X}), g(\mathbf{X}) \rangle_{\mathbf{X}}$  of the observable  $g$  can be described as

$$\begin{aligned} \frac{d}{dt}\langle g \rangle_s &= \left\langle \frac{\partial}{\partial t}p(\mathbf{X}), g(\mathbf{X}) \right\rangle_{\mathbf{X}} = \langle L_{\mathbf{X}}p(\mathbf{X}), g(\mathbf{X}) \rangle_{\mathbf{X}} \\ &= \langle p(\mathbf{X}), L_{\mathbf{X}}^*g(\mathbf{X}) \rangle_{\mathbf{X}} = \left\langle p(\mathbf{X}), \frac{\partial}{\partial t}g(\mathbf{X}) \right\rangle_{\mathbf{X}}, \end{aligned} \quad (11)$$

where  $g(\mathbf{X})$  remains constant and  $p(\mathbf{X})$  evolves in the second expression, while  $p(\mathbf{X})$  remains constant and  $g(\mathbf{X})$  evolves in the last expression.

The backward Fokker-Planck operator  $L_{\mathbf{X}}^*$  in Eq. (10) serves as the infinitesimal generator of the stochastic Koopman operator for Eq. (6)<sup>51,52</sup>. We can easily confirm that, in the noiseless limit  $\mathbf{D}(\mathbf{X}) \rightarrow 0$ , the backward Fokker-Planck operator  $L_{\mathbf{X}}^*$  goes back to the linear operator  $A_c = \mathbf{A}(\mathbf{X}) \cdot \nabla$ , i.e., the infinitesimal generator of the Koopman operator for the deterministic system in Eq. (1) (see the details in Appendix A and Ref.<sup>54</sup>).

The linear differential operators  $L_{\mathbf{X}}$  and  $L_{\mathbf{X}}^*$  possess a biorthogonal eigensystem  $\{\lambda_k, P_k, Q_k\}_{k=0,1,2,\dots}$  consisting of the eigenvalue  $\lambda_k$  and eigenfunctions  $P_k(\mathbf{X})$  and  $Q_k(\mathbf{X})$ , satisfying

$$\begin{aligned} L_{\mathbf{X}}P_k(\mathbf{X}) &= \lambda_k P_k(\mathbf{X}), \quad L_{\mathbf{X}}^*Q_k(\mathbf{X}) = \overline{\lambda_k}Q_k(\mathbf{X}), \\ \langle P_k(\mathbf{X}), Q_l(\mathbf{X}) \rangle_{\mathbf{X}} &= \delta_{kl}, \end{aligned} \quad (12)$$

where  $k, l = 0, 1, 2, \dots$ , and  $\delta_{kl}$  represents the Kronecker delta<sup>57</sup>.

We assume that, among the eigenvalues, one eigenvalue  $\lambda_0$  equals zero, which is associated with the stationary state  $p_0(\mathbf{X})$  of the system, i.e.,  $L_{\mathbf{X}}p_0(\mathbf{X}) = 0$ , and all other eigenvalues possess negative real parts. We also assume that the eigenvalues with the largest non-vanishing real part (or equivalently the smallest absolute real part, i.e., the slowest decay rate) form a complex-conjugate pair, denoted by

$$\lambda_1 = \mu_s - i\Omega_s, \quad \overline{\lambda_1} = \mu_s + i\Omega_s, \quad (13)$$

where  $|\mu_s|$  ( $\mu_s < 0$ ) represents the decay rate and  $\Omega_s = \text{Im } \overline{\lambda_1}$  represents the frequency of the fundamental oscillation. With these assumptions, the oscillatory property of the system is embodied. In general, we obtain a branch of complex-conjugate eigenvalues of  $L_{\mathbf{x}}^*$  in addition to the above slowest-decaying fundamental mode, but we do not consider those modes because their imaginary parts are essentially integer multiples of  $\Omega_s$  and are related to the fundamental mode. Regarding the asymptotic amplitude, we select a non-zero eigenvalue with the largest real part that is not included in the above branch as the independent, second-slowest decaying mode (see also Fig. 1(a) and the colored schematic diagram in Fig. 5 in Appendix B). We note that this eigenvalue may be a complex value when  $N \geq 3$ , but we focus on the case  $N = 2$ , for correspondence with the scenario of the quantum quasiprobability distribution discussed later in Sec. III B, and assume that this eigenvalue lies on the real axis. Thus, we consider that the largest non-zero eigenvalue on the real axis, denoted by  $\kappa_s = \lambda_2$ , characterizes the decay rate of the asymptotic amplitude of the system, i.e., the deviation of the system state from the averaged oscillatory state.

The stochastic asymptotic phase of the system in Eq. (6) is defined, on the basis of the relationship with the stochastic Koopman operator theory, as the argument of the eigenfunction  $Q_1(\mathbf{X})$  of  $L_{\mathbf{X}}^*$  associated with  $\overline{\lambda_1}$ , expressed as

$$\Phi_s(\mathbf{X}) = \arg Q_1(\mathbf{X}). \quad (14)$$

The exponential average of  $\Phi_s$  satisfies<sup>49,54</sup>

$$\begin{aligned} \frac{d}{dt} \arg \mathbb{E}^{\mathbf{X}_0} [e^{i\Phi_s(\mathbf{X}(t))}] &= \frac{d}{dt} \arg \mathbb{E}^{\mathbf{X}_0} [Q_1(\mathbf{X}(t))] \\ &= \text{Im} \overline{\lambda_1} = \Omega_s, \end{aligned} \quad (15)$$

where  $\mathbb{E}^{\mathbf{X}_0}$  represents the average over the stochastic trajectories of Eq. (6) originating from an initial point  $\mathbf{X}_0 \in \mathbb{R}^N$ . Thus,  $\phi(t, \mathbf{X}_0) = \arg \mathbb{E}^{\mathbf{X}_0} [e^{i\Phi_s(\mathbf{X}(t))}]$  satisfies  $\phi(t, \mathbf{X}_0) = \Omega_s t + \phi(0, \mathbf{X}_0)$

Likewise, the stochastic asymptotic amplitude of the system in Eq. (6) is defined as the eigenfunction  $Q_2(\mathbf{X})$  of  $L_{\mathbf{X}}^*$  associated with the largest non-zero real eigenvalue  $\kappa_s (= \lambda_2)$  as

$$R_s(\mathbf{X}) = Q_2(\mathbf{X}). \quad (16)$$

The average of  $R_s(\mathbf{X})$  satisfies<sup>50,54</sup>

$$\frac{d}{dt}\mathbb{E}^{\mathbf{X}_0}[R_s(\mathbf{X}(t))] = \frac{d}{dt}\mathbb{E}^{\mathbf{X}_0}[Q_2(\mathbf{X}(t))] = \kappa_s\mathbb{E}^{\mathbf{X}_0}[Q_2(\mathbf{X}(t))] = \kappa_s\mathbb{E}^{\mathbf{X}_0}[R_s(\mathbf{X}(t))]. \quad (17)$$

Hence,  $r(t, \mathbf{X}_0) = \mathbb{E}^{\mathbf{X}_0}[R_s(\mathbf{X})]$  satisfies  $r(t, \mathbf{X}_0) = e^{\kappa_s t}r(0, \mathbf{X}_0)$ .

As explained above, the asymptotic phase defined by Eq. (14) increases with a constant frequency  $\Omega_s$ , and the asymptotic amplitude defined by Eq. (16) decays exponentially with a rate  $\kappa_s$ , on average with the stochastic evolution of the system. In the noiseless limit  $\mathbf{D}(\mathbf{X}) \rightarrow 0$ ,  $\overline{\lambda_1} = u_s + i\Omega_s$  and  $\lambda_2 = \kappa_s$  approach  $\Lambda_0 = i\Omega_c$  and  $\Lambda_1 = \kappa_c$ , respectively, and the above stochastic definitions coincide with the deterministic definitions (see also the colored schematic diagram in Fig. 5 in Appendix B). Therefore, these phase and amplitude functions for stochastic oscillatory systems can be considered as a natural extension of the deterministic asymptotic phase and amplitude in Eqs. (4) and (5) from the Koopman operator viewpoint. It is noted that we may also select the eigenvalue  $\lambda_1$  and eigenfunction  $\overline{Q_1(\mathbf{X})}$  to define the stochastic asymptotic phase, which reverses its direction of increase.

### III. ASYMPTOTIC PHASE AND AMPLITUDE FOR QUANTUM OSCILLATORY SYSTEMS

Our aim in this study is to propose the asymptotic amplitude for quantum oscillatory systems. In Ref.<sup>35</sup>, we have introduced a quantum mechanical definition of the asymptotic phase for quantum oscillatory systems by extending classical definitions of the asymptotic phase, shown in Sec. II, from the Koopman operator viewpoint. In a similar manner, we can introduce a quantum asymptotic amplitude by extending the classical asymptotic amplitude, shown in Sec. II. In this section, we give a brief overview of quantum oscillatory systems, review the quantum asymptotic phase in Ref.<sup>35</sup>, and introduce a definition of the quantum asymptotic amplitude. In what follows, we use standard notations for open quantum systems without a detailed explanation (see, e.g., Refs.<sup>58–60</sup> for further details).

#### A. Quantum oscillatory systems

Consider a quantum oscillatory system with a single degree of freedom coupled to reservoirs. Under the assumption that the interactions of the system with the reservoirs are

instantaneous and a Markovian approximation can be employed, the time evolution of the system's density operator  $\rho$  obeys the quantum master equation<sup>58,59</sup>,

$$\dot{\rho} = \mathcal{L}\rho = -i[H, \rho] + \sum_{j=1}^n \mathcal{D}[C_j]\rho, \quad (18)$$

where  $\mathcal{L}$  is a Liouville superoperator governing the evolution of  $\rho$ ,  $H$  denotes a system Hamiltonian,  $C_j$  denotes a coupling operator between the system and the  $j$ th reservoir ( $j = 1, \dots, n$ ),  $[A, B] = AB - BA$  denotes the commutator,  $\mathcal{D}[C]\rho = C\rho C^\dagger - (\rho C^\dagger C + C^\dagger C\rho)/2$  denotes the Lindblad form ( $\dagger$  denotes Hermitian conjugate), and we set the reduced Planck's constant as  $\hbar = 1$ .

We introduce an inner product  $\langle X, Y \rangle_{tr} = \text{Tr}(X^\dagger Y)$  of linear operators  $X$  and  $Y$  and define the superoperator  $\mathcal{L}^*$  of  $\mathcal{L}$  such that it satisfies  $\langle \mathcal{L}^* X, Y \rangle_{tr} = \langle X, \mathcal{L} Y \rangle_{tr}$ , which is explicitly expressed as

$$\mathcal{L}^* X = i[H, X] + \sum_{j=1}^n \mathcal{D}^*[C_j]X, \quad (19)$$

where  $\mathcal{D}^*[C]X = C^\dagger X C - (X C^\dagger C + C^\dagger C X)/2$  is the adjoint Lindblad form.

The superoperator  $\mathcal{L}^*$  characterizes the evolution of an observable  $F$  as

$$\dot{F} = \mathcal{L}^* F. \quad (20)$$

In the Schrödinger picture, the density operator  $\rho$  evolves according to Eq. (18), while the observation operator  $F$  remains constants. Conversely, in the Heisenberg picture,  $F$  evolves according to Eq. (20), while  $\rho$  remains constant. The expectation value

$$\langle F \rangle_q = \text{Tr}(\rho F) = \langle \rho, F \rangle_{tr} \quad (21)$$

of  $F$  with respect to  $\rho$  remains the same in both pictures (note that  $\rho$  is self-adjoint).

The evolution of the expectation value Eq.(21) is expressed as

$$\frac{d}{dt} \langle F \rangle_q = \langle \mathcal{L}\rho, F \rangle_{tr} = \langle \rho, \mathcal{L}^* F \rangle_{tr}, \quad (22)$$

where  $F$  remains constant and  $\rho$  evolves in the second expression (Schrödinger picture), while  $\rho$  remains constant and  $F$  evolves in the last expression (Heisenberg picture). The time evolution of the expectation of the observable for quantum systems in Eq. (22) is analogous to that for classical stochastic systems in Eq. (11). Thus, the adjoint operator  $\mathcal{L}^*$

corresponds to the backward Fokker-Planck operator  $L_{\mathbf{X}}^*$ , or equivalently, to the infinitesimal generator of the Koopman operator  $A_c$ , in Sec. II<sup>35</sup>.

The Liouville superoperator  $\mathcal{L}$  possesses a biorthogonal eigensystem  $\{\Lambda_k, U_k, V_k\}_{k=0,1,2,\dots}$  consisting of the eigenvalue  $\Lambda_k$  and eigenoperators  $U_k$  and  $V_k$ , satisfying

$$\mathcal{L}U_k = \Lambda_k U_k, \quad \mathcal{L}^*V_k = \overline{\Lambda_k} V_k, \quad \langle V_k, U_l \rangle_{tr} = \delta_{kl}, \quad (23)$$

for  $k, l = 0, 1, 2, \dots$

We assume that, among eigenvalues, one eigenvalue  $\Lambda_0$  equals zero, which is associated with the stationary state  $\rho_0$  of the system, i.e.,  $\mathcal{L}\rho_0 = 0$ , and all other eigenvalues possess negative real parts. This assumption also means the absence of decoherence-free subspaces<sup>61</sup>. Additionally, we assume that the eigenvalues with the largest non-vanishing real part (or equivalently the smallest absolute real part, i.e., the slowest decay rate) form a complex-conjugate pair, denoted by

$$\Lambda_1 = \mu_q - i\Omega_q, \quad \overline{\Lambda_1} = \mu_q + i\Omega_q, \quad (24)$$

where  $|\mu_q|$  ( $\mu_q < 0$ ) represents the decay rate and  $\Omega_q = \text{Im } \overline{\Lambda_1}$  represents the frequency of the fundamental oscillation. With these assumptions, the oscillatory property of the system is embodied. Analogous to the stochastic case, for the asymptotic amplitude, we select the largest non-zero eigenvalue on the real axis, denoted by  $\kappa_q = \Lambda_2$ , considering it characterizes the decay rate of the asymptotic amplitude of the system.

## B. Phase-space representation

We can transform the density operator  $\rho$  into a quasiprobability distribution on the phase space<sup>58,59,62</sup>. Employing the  $P$ -representation<sup>58,59,62</sup>, we express  $\rho$  as

$$\rho = \int p(\boldsymbol{\alpha}) |\alpha\rangle \langle \alpha| d\boldsymbol{\alpha}, \quad (25)$$

where  $|\alpha\rangle$  represents a coherent state specified by a complex value  $\alpha$ , or equivalently by a complex vector  $\boldsymbol{\alpha} = (\alpha, \bar{\alpha})^T$ ,  $p(\boldsymbol{\alpha})$  represents a quasiprobability distribution of  $\boldsymbol{\alpha}$ ,  $d\boldsymbol{\alpha} = d\alpha d\bar{\alpha}$ , and the integral is taken over the entire complex plane.

Similarly, we transform the observable  $F$  into a function in the phase space as

$$f(\boldsymbol{\alpha}) = \langle \alpha | F | \alpha \rangle, \quad (26)$$

where we arrange the operator  $F$  in the normal order<sup>58,59,62</sup>. By introducing the  $L^2$  inner product  $\langle g(\boldsymbol{\alpha}), h(\boldsymbol{\alpha}) \rangle_{\alpha} = \int \overline{g(\boldsymbol{\alpha})} h(\boldsymbol{\alpha}) d\boldsymbol{\alpha}$  of two functions  $g(\boldsymbol{\alpha})$  and  $h(\boldsymbol{\alpha})$ , the expectation value of  $F$  with respect to  $\rho$  is expressed as

$$\langle F \rangle_q = \text{Tr}(\rho F) = \int d\boldsymbol{\alpha} p(\boldsymbol{\alpha}) f(\boldsymbol{\alpha}) = \langle p(\boldsymbol{\alpha}), f(\boldsymbol{\alpha}) \rangle_{\alpha}. \quad (27)$$

The time evolution of  $p(\boldsymbol{\alpha})$  corresponding to Eq. (18) is described by a partial differential equation

$$\partial_t p(\boldsymbol{\alpha}) = L_{\alpha} p(\boldsymbol{\alpha}), \quad (28)$$

where the differential operator  $L_{\alpha}$  satisfies  $\mathcal{L}\rho = \int L_{\alpha} p(\boldsymbol{\alpha}) |\alpha\rangle \langle \alpha| d\boldsymbol{\alpha}$ . The explicit form of  $L_{\alpha}$  can be derived from Eq. (18) via the standard calculus for the phase-space representation<sup>58,59</sup>. The corresponding evolution of  $f(\boldsymbol{\alpha})$  in the Heisenberg picture is also described as

$$\partial_t f(\boldsymbol{\alpha}) = L_{\alpha}^+ f(\boldsymbol{\alpha}), \quad (29)$$

where the differential operator  $L_{\alpha}^+$  is the adjoint of  $L_{\alpha}$  with respect to the  $L^2$  inner product, i.e.,  $\langle L_{\alpha}^+ g(\boldsymbol{\alpha}), h(\boldsymbol{\alpha}) \rangle_{\alpha} = \langle g(\boldsymbol{\alpha}), L_{\alpha} h(\boldsymbol{\alpha}) \rangle_{\alpha}$ , which satisfies  $L_{\alpha}^+ f(\boldsymbol{\alpha}) = \langle \alpha | \mathcal{L}^* F | \alpha \rangle$ .

The differential operator  $L_{\alpha}$  possesses a biorthogonal eigensystem  $\{\Lambda_k, U_k, V_k\}_{k=0,1,2,\dots}$  consisting of the eigenvalue  $\Lambda_k$  and eigenfunctions  $u_k(\boldsymbol{\alpha})$  and  $v_k(\boldsymbol{\alpha})$ , satisfying

$$L_{\alpha} u_k = \Lambda_k u_k, \quad L_{\alpha}^+ v_k = \overline{\Lambda_k} v_k, \quad \langle v_k, u_l \rangle_{\alpha} = \delta_{kl}. \quad (30)$$

This eigensystem has a one-to-one correspondence with Eq. (23). The eigenvalues  $\{\Lambda_k\}_{k \geq 0}$  are identical to those of  $\mathcal{L}$ . The eigenfunctions  $u_k$  and  $v_k$  of  $L_{\alpha}$  and  $L_{\alpha}^+$  are linked to the eigenoperators  $U_k$  and  $V_k$  of  $\mathcal{L}$  and  $\mathcal{L}^*$  as

$$U_k = \int u_k(\boldsymbol{\alpha}) |\alpha\rangle \langle \alpha| d\boldsymbol{\alpha}, \quad v_k(\boldsymbol{\alpha}) = \langle \alpha | V_k | \alpha \rangle, \quad (31)$$

which are derived from  $\mathcal{L}U_k = \int u_k(\boldsymbol{\alpha}) \{\mathcal{L}|\alpha\rangle \langle \alpha|\} d\boldsymbol{\alpha} = \int \{L_{\alpha} u_k(\boldsymbol{\alpha})\} |\alpha\rangle \langle \alpha| d\boldsymbol{\alpha} = \int \Lambda_k u_k(\boldsymbol{\alpha}) |\alpha\rangle \langle \alpha| d\boldsymbol{\alpha} = \Lambda_k U_k$  and  $L_{\alpha}^+ v_k = L_{\alpha}^+ \langle \alpha | V_k | \alpha \rangle = \langle \alpha | \mathcal{L}^* V_k | \alpha \rangle = \overline{\Lambda_k} \langle \alpha | V_k | \alpha \rangle = \overline{\Lambda_k} v_k$ .

### C. Quantum asymptotic phase

Before introducing the quantum asymptotic amplitude, we give a brief overview of the quantum asymptotic phase, which is introduced in Ref.<sup>35</sup> by extending the classical definitions of the asymptotic phase, shown in Sec. II, on the basis of the Koopman operator

theory. We note that, in quantum systems, the system state is described by the density operator  $\rho$  and the description of individual trajectories as in the classical stochastic systems cannot be taken.

First, we introduce the quantum asymptotic phase  $\Phi_q(\boldsymbol{\alpha})$  of the coherent state  $\boldsymbol{\alpha}$  in the  $P$  representation. Considering the definition of the asymptotic phase in terms of the eigenfunction  $Q_1(\mathbf{X})$  of the backward Fokker-Planck operator  $L_{\mathbf{X}}^*$  in the classical stochastic case, we introduce the definition of the quantum asymptotic phase  $\Phi_q(\boldsymbol{\alpha})$  as the argument of the complex conjugate of the eigenfunction  $v_1(\boldsymbol{\alpha})$  in the  $P$  representation associated with the principal eigenvalue  $\bar{\Lambda}_1$  as

$$\Phi_q(\boldsymbol{\alpha}) = \arg v_1(\boldsymbol{\alpha}) = \arg \langle \alpha | V_1 | \alpha \rangle. \quad (32)$$

Next, for the general quantum state  $\rho$ , which can be represented as a superposition of coherent states with the weight  $p(\boldsymbol{\alpha})$ , as given in Eq. (25), we introduce the definition of the asymptotic phase of  $\rho$  as

$$\Phi_q(\rho) = \arg \langle p(\boldsymbol{\alpha}), v_1(\boldsymbol{\alpha}) \rangle_{\boldsymbol{\alpha}} = \arg \langle \rho, V_1 \rangle_{tr}. \quad (33)$$

It can be verified that the asymptotic phase  $\Phi_q(\rho)$  evolves with a constant frequency  $\Omega_q$  when the quantum state  $\rho$  evolves according to the quantum master equation (18).

Introducing

$$\Psi_q(\rho) = \langle p(\boldsymbol{\alpha}), v_1(\boldsymbol{\alpha}) \rangle_{\boldsymbol{\alpha}} = \langle \rho, V_1 \rangle_{tr}, \quad (34)$$

we obtain the time evolution of this function as follows

$$\begin{aligned} \frac{d}{dt} \Psi_q(\rho) &= \left\langle \frac{\partial p(\boldsymbol{\alpha})}{\partial t}, v_1(\boldsymbol{\alpha}) \right\rangle_{\boldsymbol{\alpha}} = \langle L_{\boldsymbol{\alpha}} p(\boldsymbol{\alpha}), v_1(\boldsymbol{\alpha}) \rangle_{\boldsymbol{\alpha}} = \langle p(\boldsymbol{\alpha}), L_{\boldsymbol{\alpha}}^* v_1(\boldsymbol{\alpha}) \rangle_{\boldsymbol{\alpha}} \\ &= \langle p(\boldsymbol{\alpha}), \bar{\Lambda}_1 v_1(\boldsymbol{\alpha}) \rangle_{\boldsymbol{\alpha}} = \bar{\Lambda}_1 \langle p(\boldsymbol{\alpha}), v_1(\boldsymbol{\alpha}) \rangle_{\boldsymbol{\alpha}} = \bar{\Lambda}_1 \Psi_q(\rho), \end{aligned} \quad (35)$$

or equivalently,

$$\begin{aligned} \frac{d}{dt} \Psi_q(\rho) &= \langle \dot{\rho}, V_1 \rangle_{tr} = \langle \mathcal{L} \rho, V_1 \rangle_{tr} = \langle \rho, \mathcal{L}^* V_1 \rangle_{tr} \\ &= \langle \rho, \bar{\Lambda}_1 V_1 \rangle_{tr} = \bar{\Lambda}_1 \langle \rho, V_1 \rangle_{tr} = \bar{\Lambda}_1 \Psi_q(\rho). \end{aligned} \quad (36)$$

Integrating by time, we obtain

$$\Psi_q(\rho) = \exp(\bar{\Lambda}_1 t) \Psi_q(\rho_0) = \exp[(\mu_q + i\Omega_q)t] \Psi_q(\rho_0), \quad (37)$$

with  $\rho_0$  representing the initial state at  $t = 0$ , which produces the asymptotic phase as

$$\Phi_q(\rho) = \arg \Psi_q(\rho) = \Omega_q t + \arg \Phi_q(\rho_0). \quad (38)$$

Differentiating with respect to time  $t$ , we obtain

$$\frac{d}{dt} \Phi_q(\rho) = \Omega_q. \quad (39)$$

Hence, the asymptotic phase  $\Phi_q(\rho)$  increases with a constant frequency  $\Omega_q$  with the evolution of the quantum state  $\rho$ .

As explained above, we can define the asymptotic phase  $\Phi_q(\rho)$  of the quantum state  $\rho$ , using the eigenfunction  $v_1(\boldsymbol{\alpha})$  of the adjoint linear operator  $L_{\boldsymbol{\alpha}}^*$ , or equivalently, the eigenoperator  $V_1$  of the adjoint operator  $\mathcal{L}^*$  associated with the eigenvalue  $\overline{\Lambda}_1$ . The quantum master equation (18), adjoint Liouville operator  $\mathcal{L}^*$  (or equivalently adjoint differential operator  $L_{\boldsymbol{\alpha}}^*$  in the  $P$  representation), and eigenoperator  $V_1$  (or equivalently the eigenfunction  $v_1(\boldsymbol{\alpha})$  in the  $P$  representation) with the eigenvalue  $\overline{\Lambda}_1$  correspond to the forward Fokker-Planck equation (7), backward Fokker-Planck operator  $L_{\mathbf{X}}^*$ , and eigenfunction  $Q_1(\mathbf{X})$  with the eigenvalue  $\overline{\lambda}_1$  in the classical stochastic system discussed in Sec. II B, respectively. As in the classical stochastic case, we may also select the eigenvalue  $\Lambda_1$ , eigenfunction  $\overline{v_1(\boldsymbol{\alpha})}$ , and eigenoperator  $V_1^\dagger$  to define the quantum asymptotic phase, which reverses its direction of increase.

It should be stressed that the system state is generally represented by the density operator  $\rho$  or quasiprobability distribution  $p(\boldsymbol{\alpha})$  and individual trajectories of the system, corresponding to the SDE in Eq. (6), cannot be considered in the quantum case.

#### D. Quantum asymptotic amplitude

The purpose of this study is to introduce a definition of the quantum asymptotic amplitude by extending the stochastic asymptotic amplitude discussed in Sec. II, in a similar way to define the quantum asymptotic phase. First, we introduce the quantum asymptotic amplitude  $R_q(\boldsymbol{\alpha})$  of the coherent state  $\boldsymbol{\alpha}$  in the  $P$  representation. Considering the definition of the asymptotic amplitude in Eq. (16) in terms of the eigenfunction  $Q_2(\mathbf{X})$  of the backward Fokker-Planck operator  $L_{\mathbf{X}}^*$  in the classical stochastic case, we define the quantum asymptotic amplitude  $R_q(\boldsymbol{\alpha})$  as the eigenfunction  $v_2(\boldsymbol{\alpha})$  in the  $P$  representation associated

with the largest non-zero real eigenvalue  $\kappa_q(= \Lambda_2)$  as

$$R_q(\boldsymbol{\alpha}) = v_2(\boldsymbol{\alpha}) = \langle \boldsymbol{\alpha} | V_2 | \boldsymbol{\alpha} \rangle. \quad (40)$$

Next, for a given quantum state  $\rho$ , which is represented as a superposition of coherent states with the weight  $p(\boldsymbol{\alpha})$  in Eq. (25), we define the asymptotic amplitude of  $\rho$  as

$$R_q(\rho) = \langle p(\boldsymbol{\alpha}), v_2(\boldsymbol{\alpha}) \rangle_{\boldsymbol{\alpha}} = \langle \rho, V_2 \rangle_{tr}. \quad (41)$$

We can confirm that the asymptotic amplitude  $R_q(\rho)$  evolves with a constant rate  $\kappa_q$  when the quantum state  $\rho$  evolves according to the quantum master equation (18).

$$\begin{aligned} \frac{d}{dt} R_q(\rho) &= \left\langle \frac{\partial p(\boldsymbol{\alpha})}{\partial t}, v_2(\boldsymbol{\alpha}) \right\rangle_{\boldsymbol{\alpha}} = \langle L_{\boldsymbol{\alpha}} p(\boldsymbol{\alpha}), v_2(\boldsymbol{\alpha}) \rangle_{\boldsymbol{\alpha}} = \langle p(\boldsymbol{\alpha}), L_{\boldsymbol{\alpha}}^* v_2(\boldsymbol{\alpha}) \rangle_{\boldsymbol{\alpha}} \\ &= \langle p(\boldsymbol{\alpha}), \kappa_q v_2(\boldsymbol{\alpha}) \rangle_{\boldsymbol{\alpha}} = \kappa_q \langle p(\boldsymbol{\alpha}), v_2(\boldsymbol{\alpha}) \rangle_{\boldsymbol{\alpha}} = \kappa_q R_q(\rho), \end{aligned} \quad (42)$$

or equivalently,

$$\begin{aligned} \frac{d}{dt} R_q(\rho) &= \langle \dot{\rho}, V_2 \rangle_{tr} = \langle \mathcal{L}\rho, V_2 \rangle_{tr} = \langle \rho, \mathcal{L}^* V_2 \rangle_{tr} \\ &= \langle \rho, \kappa_q V_2 \rangle_{tr} = \kappa_q \langle \rho, V_2 \rangle_{tr} = \kappa_q R_q(\rho). \end{aligned} \quad (43)$$

Integrating over time, we obtain

$$R_q(\rho) = \exp(\kappa_q t) R_q(\rho_0), \quad (44)$$

where  $\rho_0$  is the initial state at  $t = 0$ . Thus, the asymptotic amplitude  $R_q(\rho)$  decays exponentially with a constant rate  $\kappa_q$  with the evolution of the quantum state  $\rho$ .

As explained above, we define the asymptotic amplitude  $R_q(\rho)$  of the quantum state  $\rho$ , using the eigenfunction  $v_2(\boldsymbol{\alpha})$  of the adjoint linear operator  $L_{\boldsymbol{\alpha}}^*$ , or equivalently the eigenoperator  $V_2$  of the adjoint operator  $\mathcal{L}^*$ , associated with the eigenvalue  $\kappa_q$ .

#### IV. NUMERICAL RESULTS

To validate the proposed quantum asymptotic amplitude, we consider the quantum van der Pol oscillator with the quantum Kerr effect, exhibiting quantum limit-cycle oscillations, both in the semiclassical and strong quantum regime. We also consider the quantum van der Pol model with the quantum squeezing, exhibiting quantum noise-induced oscillations

near the saddle-node on invariant circle (SNIC) bifurcation<sup>6,63</sup> in the classical limit, and a degenerate parametric oscillator with nonlinear damping, exhibiting quantum noise-induced oscillations near the pitchfork bifurcation<sup>6,63</sup> in the classical limit. We also analyze a damped harmonic oscillator in Appendix D.

In our numerical calculations, we approximately truncate the density operator as a large-dimensional  $N \times N$  matrix and transform it into a  $N^2$ -dimensional vector in the double-ket notation<sup>64</sup>. We can then represent the Liouville operator by a  $N^2 \times N^2$  matrix and obtain the asymptotic phase and amplitude in Eqs. (32) and (40) from the eigensystem of this matrix<sup>35</sup>.

### A. Quantum van der Pol model with quantum Kerr effect

First, we consider an example of the quantum van der Pol oscillator with the quantum Kerr effect. The quantum master equation of the system is described by<sup>15,35</sup>

$$\dot{\rho} = \mathcal{L}\rho = -i[H, \rho] + \gamma_1 \mathcal{D}[a^\dagger]\rho + \gamma_2 \mathcal{D}[a^2]\rho, \quad (45)$$

where  $a$  and  $a^\dagger$  denote annihilation and creation operators,  $H = \omega_0 a^\dagger a + K a^{\dagger 2} a^2$  is the Hamiltonian,  $\omega_0$  denotes the frequency parameter of the oscillator,  $K$  denotes the Kerr parameter, and  $\gamma_1$  and  $\gamma_2$  denote the decay rates for negative damping and nonlinear damping, respectively. Using the standard rule of calculus<sup>58,59,62</sup>, we can obtain the differential operator  $L_\alpha$  in Eq. (28), characterizing the evolution of the  $P$  representation  $p(\alpha)$  of  $\rho$ , from the Liouville operator  $\mathcal{L}$ .

#### 1. Semiclassical regime

First, we consider the system in the semiclassical regime where  $\gamma_2$  and  $K$  are sufficiently smaller than  $\gamma_1$ . In this regime, as explained in Appendix B, the quantum master equation in Eq. (45) is described by a quantum Fokker-Planck equation for  $p(\alpha)$  in Eq. (28), and the system state is approximately described by a classical stochastic system in the phase space fluctuating along a deterministic classical trajectory due to small quantum noise<sup>14,35</sup>.

In the classical limit where the quantum noise vanishes, we describe the system by a

single complex variable  $\alpha \in \mathbb{C}$ , obeying a deterministic system, given by

$$\dot{\alpha} = \left( \frac{\gamma_1}{2} - i\omega_0 \right) \alpha - (\gamma_2 + 2Ki)\bar{\alpha}\alpha^2. \quad (46)$$

This equation is the Stuart-Landau oscillator (normal form of the supercritical Hopf bifurcation)<sup>2</sup> and possesses a stable limit-cycle attractor  $\alpha_c(\phi) = r_c e^{i\phi}$ , where  $\phi = \Omega_c t + \text{const.}$  with a natural frequency  $\Omega_c = -\omega_0 - K\gamma_1/\gamma_2$  and  $r_c = \sqrt{\gamma_1/2\gamma_2}$  (therefore the quantum van der Pol model is also referred to as the quantum Stuart-Landau model in recent literature<sup>16,30</sup>). Note that the basin  $B_\chi$  of this limit cycle is the whole complex plane except for the origin.

The classical asymptotic phase  $\Phi_c$  of this system is given by<sup>35</sup>

$$\Phi_c(\boldsymbol{\alpha}) = \arg \alpha - \frac{2K}{\gamma_2} \ln \frac{|\alpha|}{r_c} + \text{const}, \quad (47)$$

and the classical asymptotic amplitude  $R_c$  of the system is calculated as<sup>54</sup>

$$R_c(\boldsymbol{\alpha}) = c_0 \left( \gamma_2 - \frac{\gamma_1}{2(x^2 + p^2)} \right), \quad (48)$$

where  $(x, p) = (\text{Re } \alpha, \text{Im } \alpha)$  and  $c_0$  is an arbitrary real variable because the scale of the asymptotic amplitude can be arbitrarily chosen. The phase satisfies  $\dot{\Phi}_c(\boldsymbol{\alpha}) = \Omega_c$ , and the amplitude satisfies  $\dot{R}_c(\boldsymbol{\alpha}) = \kappa_c R_c(\boldsymbol{\alpha})$  with  $\kappa_c = -\gamma_1$ , when  $\alpha$  evolves within  $B_\chi$  under Eq. (46).

Figure 1(a) shows the eigenvalues of  $\mathcal{L}$  near the imaginary axis, obtained numerically, where the real eigenvalue with the largest real part  $\kappa_q$  is marked with a red dot ( $\kappa_q < 0$ ) and the principal eigenvalue  $\bar{\Lambda}_1$  with the slowest decay rate is marked with a yellow dot.

Figures 1(b) and 1(c) illustrate the quantum asymptotic amplitude  $|R_q(\boldsymbol{\alpha})|$  and the corresponding asymptotic amplitude  $|R_c(\boldsymbol{\alpha})|$ , respectively. Here, both amplitude functions are scaled by a constant factor such that the maximum value of  $|R_q|$  becomes 1, and the same color map is used for illustrating both figures. In Fig. 1(c), values of  $|R_c|$  larger than 1 near the origin are illustrated in the same color. In Fig. 1(b), the red-thin line illustrates the effective quantum periodic orbit  $\chi_q = \{\boldsymbol{\alpha} | R_q(\boldsymbol{\alpha}) = 0\}$ , and in Fig. 1(c), the orange-thin line illustrates the deterministic limit cycle  $\chi_c (= \{\boldsymbol{\alpha} | R_c(\boldsymbol{\alpha}) = 0\})$  in the classical limit. The quantum asymptotic amplitude  $R_q(\rho) = \langle p(\boldsymbol{\alpha}), R_q(\boldsymbol{\alpha}) \rangle_\alpha$  of the quantum state  $\rho$  decays exponentially to zero, and in the classical limit, the quantum periodic orbit  $\chi_q$  coincides with the classical limit cycle  $\chi_c$ . Thus, in this regime with sufficiently small quantum noise, the quantum periodic orbit  $\chi_q$  closely matches the classical limit-cycle  $\chi_c$ .

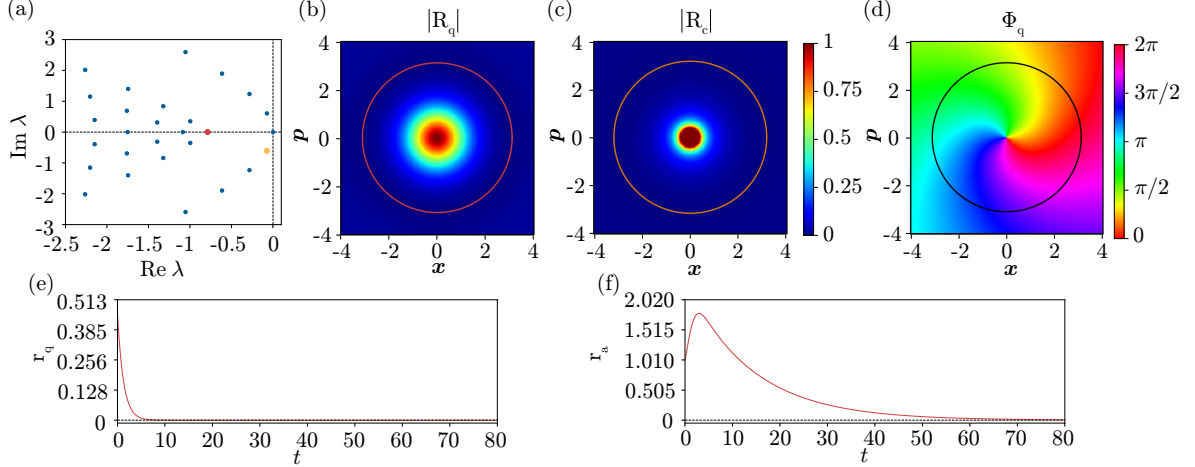


FIG. 1. Quantum asymptotic amplitude of a quantum van der Pol oscillator with the quantum Kerr effect in the semiclassical quantum regime. The parameters are  $\gamma_1 = 1$  and  $(\omega_0, \gamma_2, K)/\gamma_1 = (0.1, 0.05, 0.025)$ . (a) Eigenvalues of  $\mathcal{L}$  near the imaginary axis. The red dot represents the largest non-zero real eigenvalue  $\kappa_q$ , and the yellow dot represents the principal eigenvalue  $\overline{\Lambda_1}$  with the slowest decay rate. (b) Quantum asymptotic amplitude  $|R_q|$  with  $\kappa_q = -0.787$ . (c) Classical asymptotic amplitude  $|R_c|$  with  $\kappa_c = -1$ . (d) Quantum asymptotic phase  $\Phi_q$  with  $\Omega_q = -0.605$ . (e-f) Evolution of  $r_q$  and  $r_a$  from a pure coherent state: (e)  $r_q$ , (f)  $r_a$ . The red-thin line in (b) and the black-thin line in (d) represent the effective quantum periodic orbit  $\chi_q$ . The orange-thin line in (c) represents the deterministic limit cycle  $\chi_c$  in the classical limit. In (d),  $(x, p) = (2.5, 0)$  is chosen as the phase origin.

In Fig. 1(d), we also plot the quantum asymptotic phase  $\Phi_q(\alpha)$  with the effective quantum periodic orbit  $\chi_q$ . We see that the phase increases along the quantum orbit in the counterclockwise direction. Here, we adopt a negative value for  $\Omega_q$  so that the resulting phase  $\Phi_q$  increases in the counterclockwise direction from 0 to  $2\pi$  on the complex plane, i.e.,  $\Phi_q$  satisfies  $\oint_C \nabla \Phi_q(\mathbf{x}) \cdot d\mathbf{x} = 2\pi$  where  $\mathbf{x} = (x, p) = (\text{Re } \alpha, \text{Im } \alpha)$  and  $C$  is a circle around 0.

To validate that the quantum asymptotic amplitude yields appropriate amplitude values, we consider the free oscillatory relaxation of  $\rho$  from a initial coherent state  $\rho_0 = |\alpha_0\rangle\langle\alpha_0|$  with  $\alpha_0 = 1$  at  $t = 0$ . We evaluate  $r_q = |R_q(\rho)| = |\langle\rho, V_2\rangle_{tr}|$  of the eigenoperator  $V_2$  and compare it with  $r_a = |\langle a\rangle_q| = |\langle\rho, a\rangle_{tr}|$  of the annihilation operator  $a$ , which represents the polar radius of  $\langle a\rangle$  on the complex plane. We note that, even when the system state  $\rho$  starts from a pure coherent state, it quickly becomes a mixed state due to the coupling

with the reservoirs and eventually settles into the stationary mixed state. Figures 1(e) and 1(f) depict the evolution of  $r_q$  and  $r_a$ , respectively. The asymptotic amplitude  $r_q$  decays exponentially with a constant rate  $\kappa_q$  in Fig. 1(e). In contrast, the radius  $r_a$  does not exhibit an exponential decay over time; particularly, it increases during the transient process before  $t = 10$ , as shown in Fig. 1(f). Hence, in the semiclassical regime of the quantum van der Pol model with the quantum Kerr effect, the quantum asymptotic amplitude yields appropriate amplitude values.

## 2. *Strong quantum regime*

Next, we consider a strong quantum regime with relatively larger  $\gamma_2$  and  $K$  than  $\gamma_1$ , where only a small number of energy states take part in the system dynamics and the semiclassical model in the previous subsection is invalid.

Figure 2(a) shows the eigenvalues of  $\mathcal{L}$  near the imaginary axis, obtained numerically, with  $\kappa_q$  marked with a red dot and  $\overline{\Lambda_1}$  marked with a yellow dot.

Figures 2(b) and 2(c) depict the quantum asymptotic amplitude  $|R_q(\boldsymbol{\alpha})|$  and the corresponding asymptotic amplitude  $|R_c(\boldsymbol{\alpha})|$ , respectively, where both amplitude functions are scaled by a constant factor such that the maximum value of  $|R_q|$  becomes 1, the same color map is used for illustrating both figures, and values of  $|R_c|$  larger than 1 near the origin in Fig. 2(c) are illustrated in the same color. Also, the effective quantum periodic orbit  $\chi_q$  and the deterministic limit cycle  $\chi_c$  in the classical limit are plotted by the red-thin line in Fig. 2(b) and the orange-thin line in Fig. 2(c), respectively. In the strong quantum regime, the quantum periodic orbit  $\chi_q$  is distinctly different from the classical limit cycle  $\chi_c$ .

In Fig. 2(d), we also plot the quantum asymptotic phase  $\Phi_q(\boldsymbol{\alpha})$  with the effective quantum periodic orbit  $\chi_q$ . Here, we adopt a negative value for  $\Omega_q$  so that the resulting phase  $\Phi_q$  increases in the counterclockwise direction. We see that the phase increases along the quantum periodic orbit in the counterclockwise direction.

We consider the free oscillatory relaxation of  $\rho$  from a coherent initial state  $\rho_0 = |\alpha_0\rangle\langle\alpha_0|$  with  $\alpha_0 = 1$  at  $t = 0$  and evaluate the evolution of the asymptotic amplitude  $r_q$  and radius  $r_a$ . Figures 2(e) and (f) show the evolution of  $r_q$  and  $r_a$ , respectively. As expected, the asymptotic amplitude  $r_q$  exhibits an exponential decay with a constant rate  $\kappa_q$ . In contrast, the radius  $r_a$  does not decay exponentially but instead oscillates rapidly with time. This

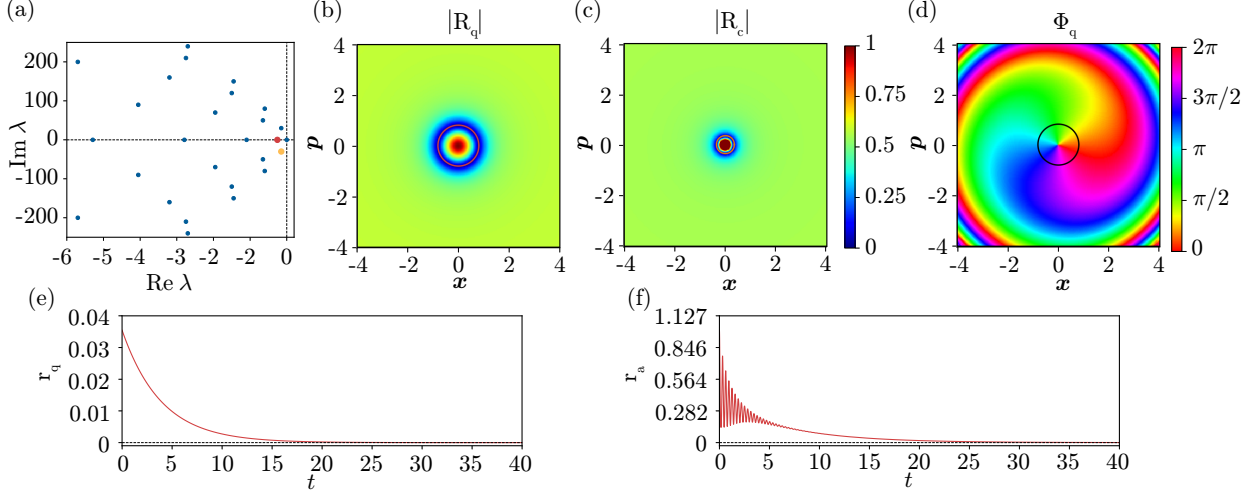


FIG. 2. Quantum asymptotic amplitude of a quantum van der Pol oscillator with the quantum Kerr effect in the strong quantum regime. The parameters are  $\gamma_1 = 0.1$  and  $(\omega_0, \gamma_2, K)/\gamma_1 = (300, 4, 100)$ . (a) Eigenvalues of  $\mathcal{L}$  near the imaginary axis. The red dot represents the largest non-zero real eigenvalue  $\kappa_q$ , and the yellow dot represents the principal eigenvalue  $\overline{\Lambda}_1$  with the slowest decay rate. (b) Quantum asymptotic amplitude  $|R_q|$  with  $\kappa_q = -0.256$ . (c) Classical asymptotic amplitude  $|R_c|$  with  $\kappa_c = -0.1$ . (d) Quantum asymptotic phase  $\Phi_q$  with  $\Omega_q = -30$ . (e-f) Evolution of  $r_q$  and  $r_a$  from a pure coherent state: (e)  $r_q$ , (f)  $r_a$ . The red-thin line in (b) and the black-thin line in (d) represent the effective quantum periodic orbit  $\chi_q$ . The orange-thin line in (c) represents the deterministic limit cycle  $\chi_c$  in the classical limit. In (d),  $(x, p) = (2.5, 0)$  is chosen as the phase origin.

behavior is observed because the transition between relatively a small number of energy levels dominates the system dynamics, and the discreteness of the energy spectra can take a significant role in this strong quantum regime. Thus, despite the strong quantum effect substantially altering the system dynamics from those in the classical limit, the quantum asymptotic amplitude  $R_q$  appropriately produces isostable amplitude values even in the strong quantum regime of the quantum van der Pol model with the quantum Kerr effect.

## B. Quantum van der Pol model with the quantum squeezing

Next, we consider a system exhibiting quantum noise-induced oscillations, i.e. oscillatory response excited by the quantum noise<sup>65</sup>; specifically, we consider a system in the classical limit is near an SNIC bifurcation<sup>6,63</sup>. As a minimum model exhibiting such quantum noise-induced oscillations, we consider a quantum van der Pol model subjected to the quantum squeezing<sup>12</sup>, whose deterministic system in the classical limit can be considered as an excitable bistable system slightly below the onset of spontaneous limit-cycle oscillations<sup>65</sup>.

Let  $\omega_{sq}$  denote the frequency of the pump beam of the quantum squeezing. In the rotating coordinate frame of frequency  $\omega_{sq}/2$ , the system is described by the quantum master equation<sup>12,14,65</sup>

$$\dot{\rho} = -i [-\Delta a^\dagger a + i\eta(a^2 e^{-i\theta} - a^{\dagger 2} e^{i\theta}), \rho] + \gamma_1 \mathcal{D}[a^\dagger]\rho + \gamma_2 \mathcal{D}[a^2]\rho, \quad (49)$$

where,  $\Delta = \omega_{sq}/2 - \omega_0$  is the detuning of the half frequency of the pump beam of squeezing from the system's frequency parameter and  $\eta e^{i\theta}$  ( $\eta \geq 0$ ,  $0 \leq \theta < 2\pi$ ) is the squeezing parameter.

In the classical limit where the quantum noise vanishes, the system is described by a single complex variable  $\alpha \in \mathbb{C}$ , obeying a deterministic system (see the derivation in Appendix C)

$$\dot{\alpha} = \left( \frac{\gamma_1}{2} + i\Delta \right) \alpha - \gamma_2 \bar{\alpha} \alpha^2 - 2\eta e^{i\theta} \bar{\alpha}. \quad (50)$$

Representing the complex variable  $\alpha$  using the modulus  $R$  and argument  $\phi$  as  $\alpha = R e^{i\phi}$ , we obtain the differential equations for these variables as

$$\dot{R} = \frac{\gamma_1}{2} R - \gamma_2 R^3 - 2\eta R \cos(2\phi - \theta), \quad (51)$$

$$\dot{\phi} = \Delta + 2\eta \sin(2\phi - \theta). \quad (52)$$

When the squeezing effect is present, i.e.,  $\eta \neq 0$ , the system possesses two stable fixed points for  $\Delta \leq 2\eta$  as can be seen from the equation for the argument  $\phi$  in Eq. (52). These fixed points annihilate with their unstable counterparts via an SNIC bifurcation at  $\Delta = 2\eta$ ; a stable limit-cycle arises and the argument  $\phi$  continuously increases when  $\Delta > 2\eta$ , while  $\phi$  possesses two stable fixed points and converges to either of them depending on the initial state when  $\Delta < 2\eta$ . When the system in the classical limit is slightly below the SNIC bifurcation, namely, when  $\Delta$  is slightly less than  $2\eta$ , the system can exhibit oscillatory

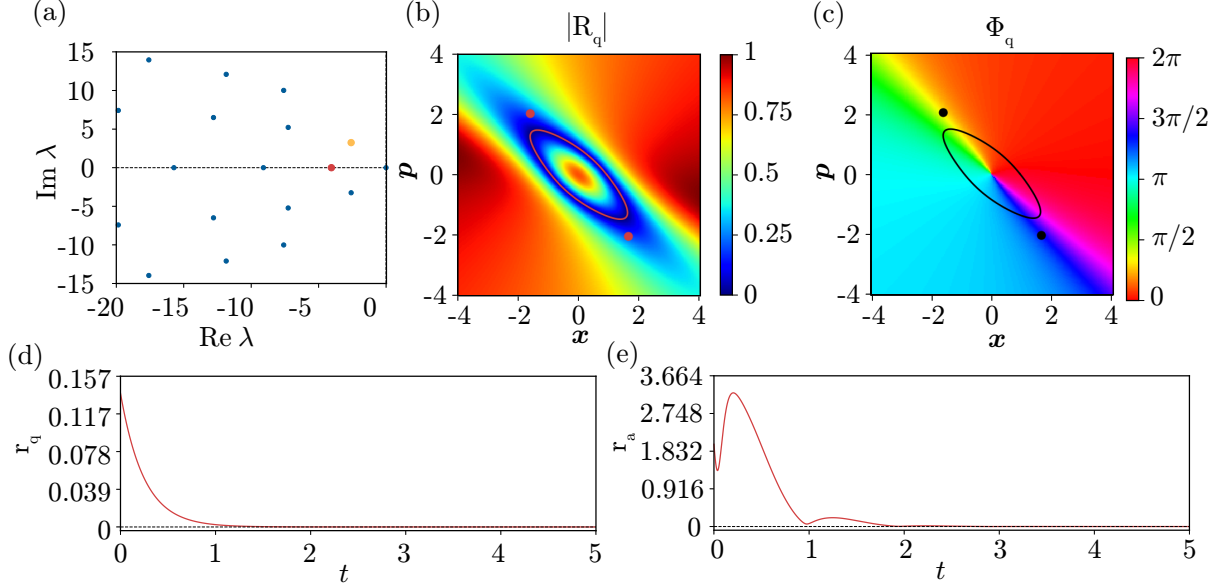


FIG. 3. Quantum asymptotic amplitude of a quatnumin van der Pol model with the quantum squeezing effect. The parameters are  $\gamma_1 = 1$  and  $(\Delta, \gamma_2, \eta)/\gamma_1 = (13.65, 0.53, 7)$ . (a) Eigenvalues of  $\mathcal{L}$  near the imaginary axis. The red dot represents the largest non-zero real eigenvalue  $\kappa_q$ , and the yellow dot represents the principal eigenvalue  $\overline{\Lambda}_1$  with the slowest decay rate. (b) Quantum asymptotic amplitude  $|R_q|$  with  $\kappa_q = -4.052$ . (c) Quantum asymptotic phase  $\Phi_q$  with  $\Omega_q = 3.248$ . (d,e) Evolution of  $r_q$  and  $r_a$  from a pure coherent state: (d)  $r_q$ , (e)  $r_a$ . The red-thin line in (b) and the black-thin line in (c) represent the effective quantum periodic orbit  $\chi_q$ , and the two red dots in (b) and the two black dots in (c) represent the two stable fixed points in the classical limit. In (c),  $(x, p) = (2.5, 0)$  is chosen as the phase origin.

response excited by the quantum noise. In what follows, we consider such a parameter configuration (see also the detail in Appendix C).

Figure 3(a) shows the eigenvalues of  $\mathcal{L}$  near the imaginary axis, obtained numerically, with  $\kappa_q$  marked with a red dot and  $\overline{\Lambda}_1$  marked with a yellow dot.

Figures 3(b) and 3(c) show the quantum asymptotic amplitude  $|R_q(\boldsymbol{\alpha})|$  and phase  $\Phi_q(\boldsymbol{\alpha})$ , respectively, where the amplitude function is scaled by a constant factor such that the maximum value of  $|R_q|$  becomes 1. Although the system in the classical limit is set below the SNIC bifurcation and only possesses two stable fixed points, which are shown by the two red dots in Fig. 3(b) and two black dots in Fig. 3(c), due to the oscillatory response excited

by the quantum noise, the effective quantum periodic orbit  $\chi_q$  arises, which is illustrated by the red-thin line in Fig. 3(b) and black-thin line in Fig. 3(c).

The quantum asymptotic phase  $\Phi_q(\boldsymbol{\alpha})$  can also be introduced by Eq. (32), which increases along the effective quantum periodic orbit  $\chi_q$ , as depicted in Fig. 3(c). Here, we adopt a positive value for  $\Omega_q$  so that the resulting phase  $\Phi_q$  increases in the counterclockwise direction from 0 to  $2\pi$  on the complex plane. The quantum asymptotic phase reflects fast-slow dynamics corresponding to the round trip between two stable fixed points, with slow dynamics (rapid phase change) near the two stable fixed points and fast dynamics (moderate phase change) between the two stable fixed points, as depicted in Fig. 3(c). It also should be noted that the asymptotic phase for a quantum noise-induced oscillation is illustrated for the first time.

We consider the free oscillatory relaxation of  $\rho$  from a coherent initial state  $\rho_0 = |\alpha_0\rangle\langle\alpha_0|$  with  $\alpha_0 = 2$  at  $t = 0$  and evaluate the evolution of the asymptotic amplitude  $r_q$  and the radius  $r_a$ . Figures 3(d) and (e) illustrate the evolution of  $r_q$  and  $r_a$ , respectively. As anticipated, the asymptotic amplitude  $r_q$  decays exponentially with a constant rate  $\kappa_q$ . In contrast, the radius  $r_a$  does not exhibit an exponential decay over time; it increases during the transient process before  $t = 2$ .

### C. A degenerate parametric oscillator with nonlinear damping

Next, we also consider a system exhibiting quantum noise-induced oscillations; particularly, we consider a system in the classical limit is near a pitchfork bifurcation<sup>66,63</sup>. As a minimum model exhibiting such quantum noise-induced oscillations, we consider a degenerate parametric oscillator with nonlinear damping<sup>66,67</sup>, whose deterministic system in the classical limit can exhibit a pitchfork bifurcation.

The pump beam of the squeezing is added also in this model. In the rotating coordinate frame with a frequency of  $\omega_{sq}/2$ , the system is described the the following quantum master equation<sup>66,67</sup>

$$\dot{\rho} = -i [-\Delta a^\dagger a + i\eta(a^2 e^{-i\theta} - a^{\dagger 2} e^{i\theta}), \rho] + \gamma_2 \mathcal{D}[a^2]\rho + \gamma_3 \mathcal{D}[a]\rho, \quad (53)$$

where  $\gamma_3$  represents the decay rate for linear damping.

In the classical limit where the quantum noise vanishes, the system is described by a single

complex variable  $\alpha \in \mathbb{C}$ , obeying a deterministic system (see the derivation in Appendix C)

$$\dot{\alpha} = \left( \frac{-\gamma_3}{2} + i\Delta \right) \alpha - \gamma_2 \bar{\alpha} \alpha^2 - 2\eta e^{i\theta} \bar{\alpha}. \quad (54)$$

Representing the complex variable  $\alpha$  using the modulus  $R$  and argument  $\phi$  as  $\alpha = R e^{i\phi}$ , we obtain the differential equations for these variables as

$$\dot{R} = \frac{-\gamma_3}{2} R - \gamma_2 R^3 - 2\eta R \cos(2\phi - \theta), \quad (55)$$

$$\dot{\phi} = \Delta + 2\eta \sin(2\phi - \theta). \quad (56)$$

When the squeezing effect is present, i.e.,  $\eta \neq 0$ , the equation for the argument in Eq. (56), possesses two stable fixed points for  $\Delta \leq 2\eta$ . In this case, a non-zero positive solution of the equation for the modulus in Eq. (55) arises via a pitchfork bifurcation at  $\eta = \frac{1}{2} \sqrt{\frac{\gamma_3^2}{4} + \Delta^2}$ ; the system possesses two stable fixed points with a common modulus when  $\eta > \frac{1}{2} \sqrt{\frac{\gamma_3^2}{4} + \Delta^2}$ , while it possesses a single stable fixed point at the origin when  $\eta \leq \frac{1}{2} \sqrt{\frac{\gamma_3^2}{4} + \Delta^2}$ .

We assume that the equation for the modulus in Eq. (55) is slightly below the bifurcation, namely  $\eta < \frac{1}{2} \sqrt{\frac{\gamma_3^2}{4} + \Delta^2}$ , and the equation for the argument in Eq. (56) is slightly below the bifurcation, namely  $\Delta < 2\eta$ . In this case, due to the effect of quantum noise, the system exceeds the pitchfork bifurcation, leading to the emergence of two stable fixed points. However, at the same time, it simultaneously exceeds the bifurcation point  $\Delta = 2\eta$  of the argument and exhibits oscillatory response of the round trip around two emerging stable fixed points, resulting in a quantum noise-induced oscillation starting from the origin. In what follows, we consider such a parameter configuration (see the details in Appendix C).

Figure 4(a) shows the eigenvalues of  $\mathcal{L}$  near the imaginary axis, obtained numerically, with  $\kappa_q$  marked with a red dot and  $\bar{\Lambda}_1$  marked with a yellow dot.

Figures 4(b) and 4(c) show the quantum asymptotic amplitude  $|R_q(\boldsymbol{\alpha})|$  and phase  $\Phi_q(\boldsymbol{\alpha})$ , respectively, where the amplitude function is scaled by a constant factor such that the maximum value of  $|R_q|$  becomes 1. Although the system in the classical limit is set below a pitchfork bifurcation and only possess a stable fixed point at the origin, which is shown by the red dot in Fig. 4(b) and black dot in in Fig. 4(c), due to the oscillatory response excited by the quantum noise, the effective quantum periodic orbit  $\chi_q$  arises, which is illustrated by the red-thin line in Fig. 4(b) and black-thin line in Fig. 4(c).

The quantum asymptotic phase  $\Phi_q(\boldsymbol{\alpha})$  can also be introduced by Eq. (32), which increases along the effective quantum periodic orbit  $\chi_q$ , as depicted in Fig. 4(c). Here, we adopt a

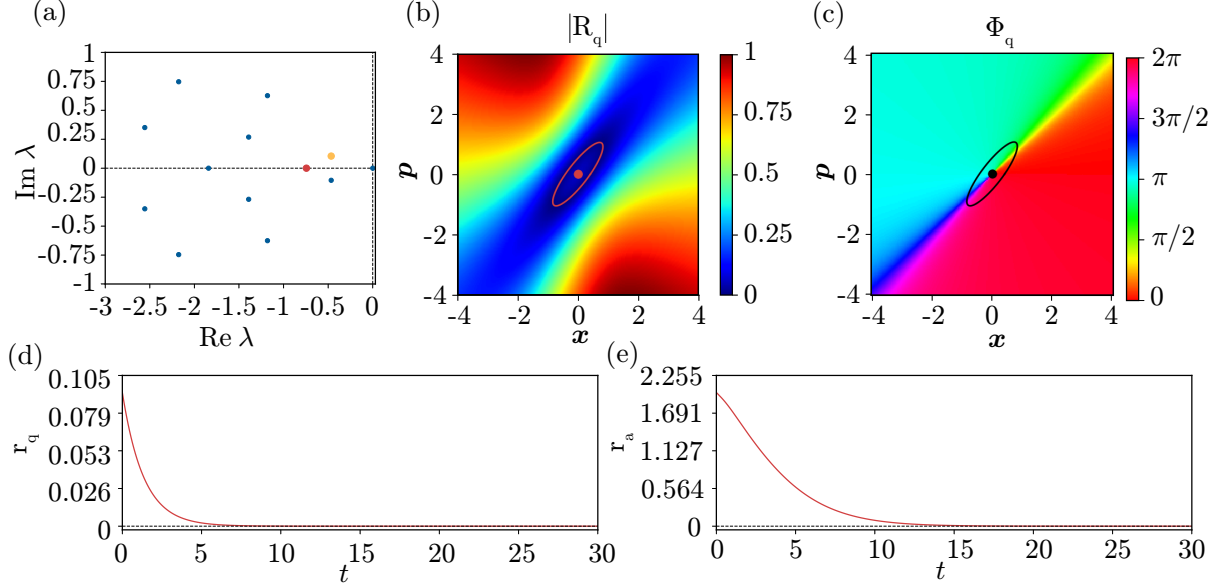


FIG. 4. Quantum asymptotic amplitude of a degenerate parametric oscillator with nonlinear damping. The parameters are  $\gamma_2 = 0.1$  and  $(\Delta, \gamma_3, \eta e^{-i\theta})/\gamma_2 = (6, 7.5, -3.25)$ . (a) Eigenvalues of  $\mathcal{L}$  near the imaginary axis. The red dot represents the largest non-zero real eigenvalue  $\kappa_q$ , and the yellow dot represents the principal eigenvalue  $\overline{\Lambda}_1$  with the slowest decay rate. (b) Quantum asymptotic amplitude  $|R_q|$  with  $\kappa_q = -0.744$ . (c) Quantum asymptotic phase  $\Phi_q$  with  $\Omega_q = 0.105$ . (d,e) Evolution of  $r_q$  and  $r_a$  from a pure coherent state: (d)  $r_q$ , (e)  $r_a$ . The red-thin line in (b) and the black-thin line in (c) represent the effective quantum periodic orbit  $\chi_q$ , and the red dot in (b) and the black dot in (c) represent the stable fixed point at the origin in the classical limit. In (c),  $(x, p) = (2.5, 0)$  is chosen as the phase origin.

positive value for  $\Omega_q$  so that the resulting phase  $\Phi_q$  increases in the counterclockwise direction. The quantum asymptotic phase reflects fast-slow dynamics, akin to that in Fig. 3(c), which corresponds to the noise-induced oscillations starting from the origin.

We consider the free oscillatory relaxation of  $\rho$  from a coherent initial state  $\rho_0 = |\alpha_0\rangle\langle\alpha_0|$  with  $\alpha_0 = 2$  at  $t = 0$  and evaluate the evolution of the asymptotic amplitude  $r_q$  and the radius  $r_a$ . Figures 4(d) and (e) illustrate the evolution of  $r_q$  and  $r_a$ , respectively. As anticipated, the asymptotic amplitude  $r_q$  decays exponentially with a constant rate  $\kappa_q$ . In contrast, the radius  $r_a$  does not exhibit an exponential decay over time.

Note that such noise-induced oscillations can also occur in classical stochastic systems

whose deterministic part is slightly below a pitchfork bifurcation. Considering the related studies on a quasicycle below a supercritical Hopf bifurcation point of the corresponding deterministic model<sup>68</sup>, we may regard this as a quasicycle below a pitchfork bifurcation point of the corresponding deterministic model.

#### D. Fundamental difference between the classical and quantum systems

A fundamental difference between the quantum asymptotic phase  $\Phi_q$  and stochastic asymptotic phase  $\Phi_s$  is discussed in Ref.<sup>35</sup>. A similar difference also exists between the quantum asymptotic amplitude  $R_q$  and stochastic asymptotic amplitude  $R_s$ .

The quantum system is characterized by the density operator, and the asymptotic amplitude  $R_q$  assigns an amplitude value to each  $\rho$ . In contrast, in the classical stochastic case, the stochastic amplitude assigns an amplitude value to each individual state  $\mathbf{X}$ , although the probability density function  $p(\mathbf{X})$  is used for calculating the stochastic asymptotic amplitude  $R_s$ . This difference arises due to the representation of the system state: a single stochastic trajectory of the noisy oscillator is described by a stochastic differential equation (SDE) in the classical stochastic case, whereas the system state is solely characterized by the density operator  $\rho$  representing the statistical state of the system in the quantum case. Indeed, we may also consider the asymptotic amplitude defined for the probability density  $p(\mathbf{X})$  rather than for the state  $\mathbf{X}$  in the classical stochastic case, which assigns an amplitude value to each  $p(\mathbf{X})$ , namely,  $R_s(p(\mathbf{X})) = \arg \int p(\mathbf{X})Q_2(\mathbf{X})d\mathbf{X}$ . Then, this stochastic asymptotic amplitude as a function of the probability density  $p(\mathbf{X})$  in the classical stochastic case corresponds to the quantum asymptotic amplitude  $R_q(\rho)$  of the density operator  $\rho$ . We considered this quantity as the average of the asymptotic amplitude values defined for individual states in Eq. (17).

In the present approach, we have only considered the asymptotic amplitude functions for quantum oscillatory systems exhibiting quantum limit-cycle oscillations and quantum noise-induced oscillations. For deterministic classical systems, asymptotic amplitudes, or isostables, can also be introduced for linear systems with stable fixed points<sup>40,42</sup>. Indeed, the quantum asymptotic amplitude can also be introduced for the quantum oscillatory systems, even if their deterministic systems in the classical limit do not exhibit or are not near the bifurcation points of nonlinear oscillations. As shown in Appendix D, we explicitly calculate

the asymptotic amplitude function of a damped quantum harmonic oscillator, which is a linear model without exhibiting nonlinear oscillations.

For deterministic classical nonlinear systems possessing a stable limit-cycle solution, the zero-level set of the asymptotic amplitude function corresponds to the limit cycle  $\chi_c$ . Hence, the effective quantum periodic orbit  $\chi_q$ , which is defined as the zero-level set of the quantum asymptotic amplitude, can be considered as a natural generalization of the limit-cycle attractor for the quantum nonlinear oscillatory systems. As shown in the examples in Sec. IV A 2, this effective quantum periodic orbit can also be defined for the system in the strong quantum regime and may be used for formulating a phase reduction theory for quantum synchronization beyond the semiclassical regime.

## V. CONCLUSIONS

In this study, we proposed a definition of the asymptotic amplitude for quantum oscillatory systems by extending the asymptotic amplitude for classical stochastic oscillatory systems from the Koopman operator viewpoint<sup>54</sup>.

Despite recent interest in quantum synchronization, a systematic analysis of quantum synchronization has been limited compared to its classical counterpart, partly due to the lack of clear definitions of phase and amplitude functions. Combined with the quantum asymptotic phase in our previous work<sup>35</sup>, the proposed definition of the asymptotic amplitude, applicable even in strong quantum regimes, may offer a promising tool for systematic and quantitative analysis of quantum synchronization.

Recently, relying on the limit-cycle trajectory obtained via the continuous measurement, a phase reduction theory for quantum nonlinear oscillators derived from the stochastic Schrodinger equation, applicable even in the strong quantum regime, has been formulated<sup>37</sup>. Leveraging the proposed phase, amplitude, and effective quantum periodic orbit, it may be possible to develop a phase and amplitude reduction theory for strongly quantum nonlinear oscillators directly derived from the quantum master equation, which simplifies the quantum oscillatory dynamics into phase and amplitude equations, facilitating detailed analysis, control, and optimization of quantum nonlinear oscillators.

## ACKNOWLEDGMENTS

The authors gratefully acknowledge stimulating discussions with Hiroya Nakao. Numerical simulations have been performed by using QuTiP numerical toolbox<sup>69,70</sup>. We acknowledge JSPS KAKENHI JP22K14274 and JST CREST JP-MJCR1913 for financial support.

## Conflict of Interest

The authors have no conflicts to disclose.

## Data availability

The data that supports the findings of this study are available within the article.

## Appendix A: Koopman operator for classical stochastic processes

In this section, we give a brief summary of the definition of the Koopman operator for classical stochastic systems described by the Ito SDE (6). For the Ito SDE (6), the stochastic Koopman operator  $U$  for an observable  $g : \mathbb{R}^N \rightarrow \mathbb{C}$  is introduced as<sup>54,71</sup>

$$U^\tau g(\mathbf{X}) = \mathbb{E}[g(S^\tau \mathbf{X})] = \int p(\mathbf{Y}, \tau | \mathbf{X}, 0) g(\mathbf{Y}) d\mathbf{Y}, \quad (\text{A1})$$

where  $S^\tau$  represents a stochastic flow of Eq. (6) and  $\mathbb{E}$  is the expectation over realizations of  $S^\tau$ . We define the infinitesimal generator of  $U^\tau$  as

$$A_s g(\mathbf{X}) = \lim_{\tau \rightarrow +0} \frac{U^\tau g(\mathbf{X}) - g(\mathbf{X})}{\tau} = \lim_{\tau \rightarrow +0} \frac{\mathbb{E}[g(S^\tau \mathbf{X})] - g(\mathbf{X})}{\tau}. \quad (\text{A2})$$

We can confirm that the backward Fokker-Planck operator  $L_{\mathbf{X}}^*$  in Eq. (10) is the infinitesimal generator of the stochastic Koopman operator<sup>54,72</sup>, namely,

$$A_s = L_{\mathbf{X}}^* = \mathbf{A}(\mathbf{X}) \frac{\partial}{\partial \mathbf{X}} + \frac{1}{2} \mathbf{D}(\mathbf{X}) \frac{\partial^2}{\partial \mathbf{X}^2}. \quad (\text{A3})$$

By employing the Itô formula<sup>57</sup>,  $g(\mathbf{X}(t))$  satisfies

$$dg(\mathbf{X}(t)) = \left( \mathbf{A}(\mathbf{X}) \frac{\partial g}{\partial \mathbf{X}} + \frac{1}{2} \mathbf{D}(\mathbf{X}) \frac{\partial^2 g}{\partial \mathbf{X}^2} \right) dt + \left( \frac{\partial g}{\partial \mathbf{X}} \right)^\top \mathbf{B}(\mathbf{X}) d\mathbf{W}(t), \quad (\text{A4})$$

and, using  $U^{dt}g(\mathbf{X}) = g(S^{dt}\mathbf{X}) = g(\mathbf{X}) + dg(\mathbf{X})$ , we obtain

$$A_s g(\mathbf{X}) = \lim_{dt \rightarrow +0} \frac{\mathbb{E}[g(\mathbf{X}) + dg(\mathbf{X})] - g(\mathbf{X})}{dt} = \mathbf{A}(\mathbf{X}) \frac{\partial g(\mathbf{X})}{\partial \mathbf{X}} + \frac{1}{2} \mathbf{D}(\mathbf{X}) \frac{\partial^2 g(\mathbf{X})}{\partial \mathbf{X}^2}, \quad (\text{A5})$$

where  $\mathbb{E}$  operates only on  $dg(\mathbf{X})$ . In the absence of noise, i.e., when  $\mathbf{D}(\mathbf{X}) = 0$ , the generator  $A_s$  will take the form  $\mathbf{A}(\mathbf{X}) \frac{\partial}{\partial \mathbf{X}} = \mathbf{A}(\mathbf{X}) \cdot \nabla$ , which coincides with the Koopman operator  $A_c$  for deterministic systems.

## Appendix B: Quantum van der Pol oscillator with the quantum Kerr effect in the semiclassical regime

In this section, we briefly explain the classical limit of the quantum van der Pol oscillator with the quantum Kerr effect. As explained in Ref.<sup>14</sup>, in the semiclassical regime, the linear operator  $L_\alpha$  in Eq. (28), which describes the evolution of the quasiprobability distribution  $p(\alpha)$  in the  $P$  representation of the quantum van der Pol oscillator, can be described by a Fokker-Planck operator

$$L_\alpha = \left[ - \sum_{j=1}^2 \partial_j \{A_j(\alpha)\} + \frac{1}{2} \sum_{j=1}^2 \sum_{k=1}^2 \partial_j \partial_k \{D_{jk}(\alpha)\} \right] \quad (\text{B1})$$

where  $\partial_1 = \partial/\partial\alpha$  and  $\partial_2 = \partial/\partial\bar{\alpha}$ .

we derive the drift vector  $\mathbf{A}(\alpha) = (A_1(\alpha), A_2(\alpha))^T \in \mathbb{C}^2$  and the matrix  $\mathbf{D}(\alpha) = (D_{jk}(\alpha)) \in \mathbb{C}^{2 \times 2}$  as

$$\mathbf{A}(\alpha) = \begin{pmatrix} \left(\frac{\gamma_1}{2} - i\omega_0\right) \alpha - (\gamma_2 + 2Ki)\bar{\alpha}\alpha^2 \\ \left(\frac{\gamma_1}{2} + i\omega_0\right) \bar{\alpha} - (\gamma_2 - 2Ki)\alpha\bar{\alpha}^2 \end{pmatrix}, \quad (\text{B2})$$

$$\mathbf{D}(\alpha) = \begin{pmatrix} -(\gamma_2 + 2Ki)\alpha^2 & \gamma_1 \\ \gamma_1 & -(\gamma_2 - 2Ki)\bar{\alpha}^2 \end{pmatrix}. \quad (\text{B3})$$

The corresponding SDE of the systems fluctuating along a deterministic classical trajectory due to small quantum noise is obtained as

$$d \begin{pmatrix} \alpha \\ \bar{\alpha} \end{pmatrix} = \begin{pmatrix} \left(\frac{\gamma_1}{2} - i\omega_0\right) \alpha - (\gamma_2 + 2Ki)\bar{\alpha}\alpha^2 \\ \left(\frac{\gamma_1}{2} + i\omega_0\right) \bar{\alpha} - (\gamma_2 - 2Ki)\alpha\bar{\alpha}^2 \end{pmatrix} dt + \boldsymbol{\beta}(\alpha) \begin{pmatrix} dW_1 \\ dW_2 \end{pmatrix}, \quad (\text{B4})$$

where  $W_1$  and  $W_2$  are independent Wiener processes, and the matrix  $\boldsymbol{\beta}(\alpha)$  is derived as

$$\boldsymbol{\beta}(\alpha) = \begin{pmatrix} \sqrt{\frac{(\gamma_1 + R_{11}(\alpha))}{2}} e^{i\chi_{11}(\alpha)/2} & -i\sqrt{\frac{(\gamma_1 - R_{11}(\alpha))}{2}} e^{i\chi_{11}(\alpha)/2} \\ \sqrt{\frac{(\gamma_1 + R_{11}(\alpha))}{2}} e^{-i\chi_{11}(\alpha)/2} & i\sqrt{\frac{(\gamma_1 - R_{11}(\alpha))}{2}} e^{-i\chi_{11}(\alpha)/2} \end{pmatrix}, \quad (\text{B5})$$

where  $R_{11}(\boldsymbol{\alpha})e^{i\chi_{11}(\boldsymbol{\alpha})} = -(\gamma_2 + 2Ki)\alpha^2$ . We note that the two equations for  $\alpha$  and  $\bar{\alpha}$  in Eq. (B4) are mutually complex conjugate and represent the same dynamics.

In the classical limit, the deterministic part of Eq. (B4) is the Stuart-Landau equation for the complex variable  $\alpha$ , given in Eq. (46), which is analytically solvable, and the asymptotic amplitude  $R_c(\boldsymbol{\alpha})$  can be explicitly obtained in Eq. (48).

By introducing a real vector  $\mathbf{X} = (\text{Re } \alpha, \text{Im } \alpha)$  and the corresponding probability density function  $p(\mathbf{X})$ , the Fokker-Planck operator  $L_\alpha$  of the form Eq. (B1) for  $p(\boldsymbol{\alpha})$  can be translated into a real Fokker-Planck operator  $L_{\mathbf{X}}$  for  $p(\mathbf{X})$  in Eq. (9).

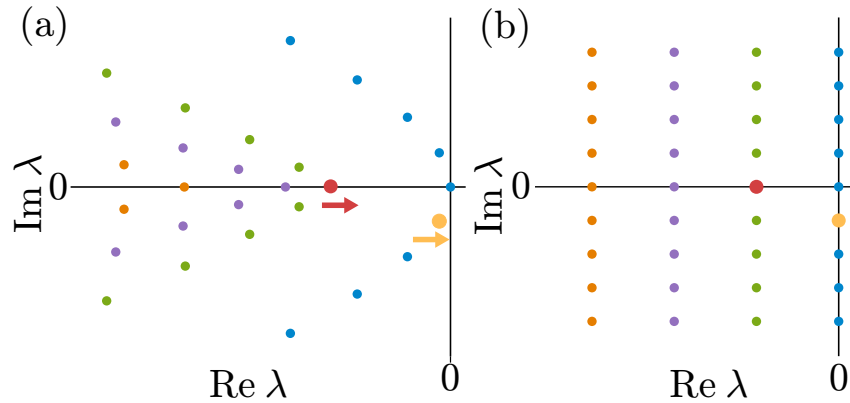


FIG. 5. A schematic diagram for eigenvalues of  $L_{\mathbf{X}}^*$  converging to the classical limit. (a) Semi-classical regime. (b) Classical limit.

Figure 5 depicts a schematic diagram illustrating the behavior of the eigenvalues of  $L_{\mathbf{X}}^*$  approaching those of the deterministic system in the classical limit possessing a stable limit-cycle solution. In the classical limit, the eigenvalues take the form  $\lambda_c = m\kappa_1 + in\omega_1$  ( $m = 0, 1, 2, \dots$  and  $n = 0, \pm 1, \pm 2$ ), where  $\kappa_1$  represents the real part of the largest non-zero eigenvalue and  $\omega_1$  represents the imaginary part of the pure-imaginary eigenvalue with the smallest absolute imaginary part. In the example of the quantum van der Pol oscillator with the quantum Kerr effect in Sec. IV A,  $\kappa_1 = -\gamma_1$  and  $\omega_1 = \Omega_c$ . When the system approaches the classical limit, each curved branch of eigenvalues of  $L_{\mathbf{X}}$  in Fig. 5(a) converges to the corresponding straight branch of eigenvalues in Fig. 5(b). The above correspondence with the conventional definition of the asymptotic phase and amplitude in the classical limit ensures the validity of our definition of the quantum asymptotic phase and amplitude.

## Appendix C: Models exhibiting noise-induced oscillations in the semiclassical regime

In this section, we briefly explain the classical limit of the models exhibiting quantum noise-induced oscillations discussed in Sec. IV B, and IV C. To discuss the models in a unified way, we consider the following quantum master equation,

$$\dot{\rho} = -i [-\Delta a^\dagger a + i\eta(a^2 e^{-i\theta} - a^{\dagger 2} e^{i\theta}), \rho] + \gamma_1 \mathcal{D}[a^\dagger] \rho + \gamma_2 \mathcal{D}[a^2] \rho + \gamma_3 \mathcal{D}[a] \rho, \quad (\text{C1})$$

In the semiclassical regime, the linear operator  $L_\alpha$  can be described by a Fokker-Planck operator in Eq. (28). The drift vector  $\mathbf{A}(\alpha) = (A_1(\alpha), A_2(\alpha))^T \in \mathbb{C}^2$  and the matrix  $\mathbf{D}(\alpha) = (D_{jk}(\alpha)) \in \mathbb{C}^{2 \times 2}$  are given by

$$\mathbf{A}(\alpha) = \begin{pmatrix} \left(\frac{\gamma_1 - \gamma_3}{2} + i\Delta\right) \alpha - \gamma_2 \bar{\alpha} \alpha^2 - 2\eta e^{i\theta} \bar{\alpha} \\ \left(\frac{\gamma_1 - \gamma_3}{2} - i\Delta\right) \bar{\alpha} - \gamma_2 \alpha \bar{\alpha}^2 - 2\eta e^{-i\theta} \bar{\alpha} \end{pmatrix}, \quad (\text{C2})$$

$$\mathbf{D}(\alpha) = \begin{pmatrix} -(\gamma_2 \alpha^2 + 2\eta e^{i\theta}) & \gamma_1 \\ \gamma_1 & -(\gamma_2 \bar{\alpha}^2 + 2\eta e^{-i\theta}) \end{pmatrix}. \quad (\text{C3})$$

The corresponding SDE of the systems fluctuating along a deterministic classical trajectory due to small quantum noise is given by

$$d \begin{pmatrix} \alpha \\ \bar{\alpha} \end{pmatrix} = \begin{pmatrix} \left(\frac{\gamma_1 - \gamma_3}{2} + i\Delta\right) \alpha - \gamma_2 \bar{\alpha} \alpha^2 - 2\eta e^{i\theta} \bar{\alpha} \\ \left(\frac{\gamma_1 - \gamma_3}{2} - i\Delta\right) \bar{\alpha} - \gamma_2 \alpha \bar{\alpha}^2 - 2\eta e^{-i\theta} \bar{\alpha} \end{pmatrix} dt + \boldsymbol{\beta}(\alpha) \begin{pmatrix} dW_1 \\ dW_2 \end{pmatrix}, \quad (\text{C4})$$

where  $W_1$  and  $W_2$  are independent Wiener processes and the matrix  $\boldsymbol{\beta}(\alpha)$  is given by

$$\boldsymbol{\beta}(\alpha) = \begin{pmatrix} \sqrt{\frac{(\gamma_1 + R_{11}(\alpha))}{2}} e^{i\chi_{11}(\alpha)/2} & -i \sqrt{\frac{(\gamma_1 - R_{11}(\alpha))}{2}} e^{i\chi_{11}(\alpha)/2} \\ \sqrt{\frac{(\gamma_1 + R_{11}(\alpha))}{2}} e^{-i\chi_{11}(\alpha)/2} & i \sqrt{\frac{(\gamma_1 - R_{11}(\alpha))}{2}} e^{-i\chi_{11}(\alpha)/2} \end{pmatrix}, \quad (\text{C5})$$

where  $R_{11}(\alpha) e^{i\chi_{11}(\alpha)} = -(\gamma_2 \alpha^2 + 2\eta e^{i\theta})$ . It is noted that the two equations for  $\alpha$  and  $\bar{\alpha}$  in Eq. (C4) are mutually complex conjugate and represent the same dynamics.

In the classical limit where the quantum noise vanishes, the system is described by a single complex variable  $\alpha \in \mathbb{C}$  obeying the deterministic part of Eq. (C5), given by

$$\dot{\alpha} = \left(\frac{\gamma_1 - \gamma_3}{2} + i\Delta\right) \alpha - \gamma_2 \bar{\alpha} \alpha^2 - 2\eta e^{i\theta} \bar{\alpha}. \quad (\text{C6})$$

Representing the complex variable  $\alpha$  using the modulus  $R$  and argument  $\phi$  as  $\alpha = Re^{i\phi}$ , we obtain the differential equations for these variables as

$$\dot{R} = \frac{\gamma_1 - \gamma_3}{2}R - \gamma_2 R^3 - 2\eta R \cos(2\phi - \theta), \quad (\text{C7})$$

$$\dot{\phi} = \Delta + 2\eta \sin(2\phi - \theta). \quad (\text{C8})$$

When  $\Delta < 2\eta$ , the equation for the argument in Eq. (C8) has two stable fixed points  $\phi_{ss} = \frac{1}{2} \left( \pi + \theta + \arcsin \left( \frac{\Delta}{2\eta} \right) \right)$  and  $\phi_{ss} + \pi$ . Additionally, when  $\gamma_1 \geq \gamma_3$ , or  $\gamma_1 < \gamma_3$  and  $\eta > \frac{1}{2} \sqrt{\frac{(\gamma_1 - \gamma_3)^2}{4} + \Delta^2}$ , the equation for the modulus  $R$  has a non zero solution  $R_{ss} = \sqrt{\frac{1}{\gamma_2} \left( \frac{\gamma_1 - \gamma_3}{2} + \sqrt{4\eta^2 - \Delta^2} \right)}$ , and consequently, the system in Eq. (C6) possesses two stable fixed points  $\alpha_{ss} = \pm R_{ss} e^{i\phi_{ss}}$ .

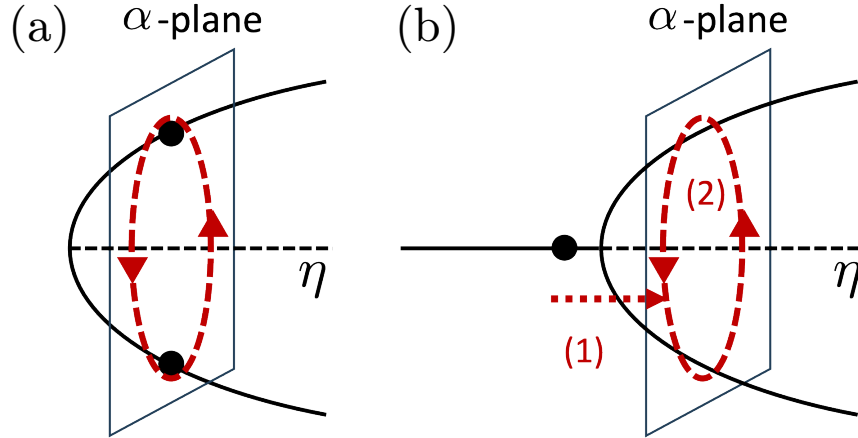


FIG. 6. A schematic diagram of noise-induced oscillations near the (a) SNIC bifurcation and (b) pitchfork bifurcation in the classical limit. In (b), the system exceeds the bifurcation points of the (1) modulus and (2) argument simultaneously.

Figs. 6 (a) and 6(b) schematically depict the bifurcation diagram when varying  $\eta$  for cases in Sec. IV B and Sec. IV C, respectively. In Sec. IV B, the equation for the argument in Eq.(C8) is slightly below the bifurcation, i.e.,  $\Delta < 2\eta$ , and the equation for the modulus in Eq.(C7) always has two stable fixed points as  $\gamma_1 > 0(= \gamma_3)$ . Then, as illustrated in Fig. 6(a), the oscillatory response of the round trip around the two stable fixed points is excited by the quantum noise. In Sec. IV C, the equation for the argument in Eq.(C8) is slightly below the bifurcation, i.e.,  $\Delta < 2\eta$ , and with  $\gamma_3 > 0(= \gamma_1)$ , the equation for

the modulus in Eq.(C7) is slightly below the bifurcation, i.e.,  $\eta < \frac{1}{2}\sqrt{\frac{(\gamma_1-\gamma_3)^2}{4} + \Delta^2}$ . Then, as illustrated in Fig. 6 (b), due to the quantum noise, the system exceeds the pitchfork bifurcation point of the modulus and two stable fixed points emerge, but at the same time, the system simultaneously exceeds the bifurcation point of the argument and exhibits the oscillatory response of the round trip around the two emerging stable fixed points. Hence, the system exhibits quantum noise-induced oscillations starting from the origin, which arises because the system simultaneously exceeds the bifurcation points of both the modulus and argument.

## Appendix D: Amplitude function of a quantum damped harmonic oscillator

In Ref.<sup>50</sup>, the stochastic asymptotic amplitude function for a classical damped harmonic oscillator described by a multi-dimensional Ornstein-Uhlenbeck process is studied. In this section, building upon their findings, we consider a simple quantum harmonic oscillator with linear damping and formally calculate the asymptotic amplitude function. Even though the system behaves linearly in the classical limit, without displaying nonlinear oscillations, we can still introduce the asymptotic amplitude function, as defined in Sec. III D.

The eigenoperator  $V_2$  of the adjoint Liouville operator  $\mathcal{L}^*$  can be analytically obtained in this case. The evolution of a damped harmonic oscillator is described by a quantum master equation

$$\dot{\rho} = \mathcal{L}\rho = -i[\omega_0 a^\dagger a, \rho] + \gamma_1 \mathcal{D}[a]\rho. \quad (\text{D1})$$

For the simplicity, we assume  $\omega_0 \neq 0$  and the system is oscillatory.

The eigenoperator associated with the largest non-zero eigenvalue on the real axis of the adjoint Liouville operator  $\mathcal{L}^*$  of  $\mathcal{L}$  is simply given by  $V_2 = a^\dagger a$ , i.e.,  $\mathcal{L}^* a^\dagger a = \kappa_q a^\dagger a$ , where  $\kappa_q = -\gamma_1$ <sup>73,74</sup>. Therefore, the asymptotic amplitude function  $R_q(\boldsymbol{\alpha})$  of the coherent state  $\boldsymbol{\alpha}$  is given by

$$R_q(\boldsymbol{\alpha}) = \langle \boldsymbol{\alpha} | a^\dagger a | \boldsymbol{\alpha} \rangle = |\boldsymbol{\alpha}|^2, \quad (\text{D2})$$

and the asymptotic amplitude function  $R_q(\rho)$  of the density operator  $\rho$  is given by

$$R_q(\rho) = \langle a^\dagger a \rangle_q = \langle \rho, a^\dagger a \rangle_{tr} \left( = \int |\boldsymbol{\alpha}|^2 p(\boldsymbol{\alpha}) d\boldsymbol{\alpha} \right). \quad (\text{D3})$$

For the initial condition  $\rho_0 = |\alpha_0\rangle\langle\alpha_0|$  with  $\alpha_0 = r_0 e^{i\theta_0}$ , the expectation of  $a^\dagger a$  evolves as

$$\frac{d}{dt}\langle a^\dagger a \rangle_q = \langle \dot{\rho}, a^\dagger a \rangle_{tr} = \langle \mathcal{L}\rho, a^\dagger a \rangle_{tr} = \langle \rho, \mathcal{L}^* a^\dagger a \rangle_{tr} = \kappa_q \langle \rho, a^\dagger a \rangle_{tr} = \kappa_q \langle a^\dagger a \rangle_q, \quad (\text{D4})$$

which yields  $\langle a^\dagger a \rangle_q = e^{\kappa_q t} \langle \rho_0, a^\dagger a \rangle_{tr} = e^{\kappa_q t} \langle \alpha_0 | a^\dagger a | \alpha_0 \rangle = e^{\kappa_q t} |\alpha_0|^2 = e^{-\gamma_1 t} r_0^2$ .

Thus, the asymptotic amplitude of the state  $\rho$  is given by

$$R_q(\rho) = e^{-\gamma_1 t} r_0^2, \quad (\text{D5})$$

which decays exponentially to zero with a constant rate  $\gamma_1$ . Thus, the zero level-set of the asymptotic amplitude forms a stable fixed point at the origin, and the effective quantum periodic orbit  $\chi_q$  is absent in this case.

As shown in this example of a quantum damped harmonic oscillator, the asymptotic amplitude function can be formally introduced for a wide class of systems, even if the system lacks nonlinear oscillatory dynamics.

## REFERENCES

- <sup>1</sup>Arthur T Winfree. The geometry of biological time. Springer, New York, 2001.
- <sup>2</sup>Yoshiki Kuramoto. Chemical oscillations, waves, and turbulence. Springer, Berlin, 1984.
- <sup>3</sup>Arkady Pikovsky, Michael Rosenblum, and Jürgen Kurths. Synchronization: a universal concept in nonlinear sciences. Cambridge University Press, Cambridge, 2001.
- <sup>4</sup>Hiroya Nakao. Phase reduction approach to synchronization of nonlinear oscillators. Contemporary Physics, 57(2):188–214, 2016.
- <sup>5</sup>G Bard Ermentrout and David H Terman. Mathematical foundations of neuroscience. Springer, New York, 2010.
- <sup>6</sup>SH Strogatz. Nonlinear dynamics and chaos. Westview Press, 1994.
- <sup>7</sup>Arif Warsi Laskar, Pratik Adhikary, Suprodip Mondal, Parag Katiyar, Sai Vinjanampathy, and Saikat Ghosh. Observation of quantum phase synchronization in spin-1 atoms. Physical Review Letters, 125(1):013601, 2020.
- <sup>8</sup>VR Krithika, Parvinder Solanki, Sai Vinjanampathy, and TS Mahesh. Observation of quantum phase synchronization in a nuclear-spin system. Physical Review A, 105(6):062206, 2022.
- <sup>9</sup>Martin Koppenhöfer, Christoph Bruder, and Alexandre Roulet. Quantum synchronization on the IBM Q system. Physical Review Research, 2(2):023026, 2020.

- <sup>10</sup>Tony E Lee and HR Sadeghpour. Quantum synchronization of quantum van der Pol oscillators with trapped ions. Physical Review Letters, 111(23):234101, 2013.
- <sup>11</sup>Stefan Walter, Andreas Nunnenkamp, and Christoph Bruder. Quantum synchronization of a driven self-sustained oscillator. Physical Review Letters, 112(9):094102, 2014.
- <sup>12</sup>Sameer Sonar, Michal Hajdušek, Manas Mukherjee, Rosario Fazio, Vlatko Vedral, Sai Vinjanampathy, and Leong-Chuan Kwek. Squeezing enhances quantum synchronization. Physical Review Letters, 120(16):163601, 2018.
- <sup>13</sup>Tony E Lee, Ching-Kit Chan, and Shenshen Wang. Entanglement tongue and quantum synchronization of disordered oscillators. Physical Review E, 89(2):022913, 2014.
- <sup>14</sup>Yuzuru Kato, Naoki Yamamoto, and Hiroya Nakao. Semiclassical phase reduction theory for quantum synchronization. Physical Review Research, 1(3):033012, 2019.
- <sup>15</sup>Niels Lörch, Ehud Amitai, Andreas Nunnenkamp, and Christoph Bruder. Genuine quantum signatures in synchronization of anharmonic self-oscillators. Physical Review Letters, 117(7):073601, 2016.
- <sup>16</sup>W-K Mok, L-C Kwek, and H Heimonen. Synchronization boost with single-photon dissipation in the deep quantum regime. Physical Review Research, 2(3):033422, 2020.
- <sup>17</sup>Dirk Witthaut, Sandro Wimberger, Raffaella Burioni, and Marc Timme. Classical synchronization indicates persistent entanglement in isolated quantum systems. Nature Communications, 8:14829, 2017.
- <sup>18</sup>Alexandre Roulet and Christoph Bruder. Quantum synchronization and entanglement generation. Physical Review Letters, 121(6):063601, 2018.
- <sup>19</sup>Niels Lörch, Simon E Nigg, Andreas Nunnenkamp, Rakesh P Tiwari, and Christoph Bruder. Quantum synchronization blockade: Energy quantization hinders synchronization of identical oscillators. Physical Review Letters, 118(24):243602, 2017.
- <sup>20</sup>Talitha Weiss, Andreas Kronwald, and Florian Marquardt. Noise-induced transitions in optomechanical synchronization. New Journal of Physics, 18(1):013043, 2016.
- <sup>21</sup>Najmeh Es' haqi Sani, Gonzalo Manzano, Roberta Zambrini, and Rosario Fazio. Synchronization along quantum trajectories. Physical Review Research, 2(2):023101, 2020.
- <sup>22</sup>Yuzuru Kato and Hiroya Nakao. Enhancement of quantum synchronization via continuous measurement and feedback control. New Journal of Physics, 23(1):013007, 2021.
- <sup>23</sup>Wenlin Li, Najmeh Es' haqi Sani, Wen-Zhao Zhang, and David Vitali. Quantum zeno effect in self-sustaining systems: Suppressing phase diffusion via repeated measurements.

- Physical Review A, 103(4):043715, 2021.
- <sup>24</sup>Yuzuru Kato and Hiroya Nakao. Semiclassical optimization of entrainment stability and phase coherence in weakly forced quantum limit-cycle oscillators. Physical Review E, 101(1):012210, 2020.
- <sup>25</sup>Michael R Hush, Weibin Li, Sam Genway, Igor Lesanovsky, and Andrew D Armour. Spin correlations as a probe of quantum synchronization in trapped-ion phonon lasers. Physical Review A, 91(6):061401, 2015.
- <sup>26</sup>Talitha Weiss, Stefan Walter, and Florian Marquardt. Quantum-coherent phase oscillations in synchronization. Physical Review A, 95(4):041802, 2017.
- <sup>27</sup>A Mari, A Farace, N Didier, V Giovannetti, and R Fazio. Measures of quantum synchronization in continuous variable systems. Physical Review Letters, 111(10):103605, 2013.
- <sup>28</sup>Minghui Xu, David A Tieri, EC Fine, James K Thompson, and Murray J Holland. Synchronization of two ensembles of atoms. Physical Review Letters, 113(15):154101, 2014.
- <sup>29</sup>Alexandre Roulet and Christoph Bruder. Synchronizing the smallest possible system. Physical Review Letters, 121(6):053601, 2018.
- <sup>30</sup>A Chia, LC Kwek, and C Noh. Relaxation oscillations and frequency entrainment in quantum mechanics. Physical Review E, 102(4):042213, 2020.
- <sup>31</sup>Lior Ben Arosh, MC Cross, and Ron Lifshitz. Quantum limit cycles and the rayleigh and van der Pol oscillators. Physical Review Research, 3(1):013130, 2021.
- <sup>32</sup>Noufal Jaseem, Michal Hajdušek, Parvinder Solanki, Leong-Chuan Kwek, Rosario Fazio, and Sai Vinjanampathy. Generalized measure of quantum synchronization. Physical Review Research, 2(4):043287, 2020.
- <sup>33</sup>Noufal Jaseem, Michal Hajdušek, Vlatko Vedral, Rosario Fazio, Leong-Chuan Kwek, and Sai Vinjanampathy. Quantum synchronization in nanoscale heat engines. Physical Review E, 101(2):020201, 2020.
- <sup>34</sup>Albert Cabot, Gian Luca Giorgi, and Roberta Zambrini. Metastable quantum entrainment. New Journal of Physics, 23(10):103017, 2021.
- <sup>35</sup>Yuzuru Kato and Hiroya Nakao. A definition of the asymptotic phase for quantum nonlinear oscillators from the Koopman operator viewpoint. Chaos: An Interdisciplinary Journal of Nonlinear Science, 32(6):063133, 2022.
- <sup>36</sup>Yuzuru Kato and Hiroya Nakao. Quantum asymptotic phases reveal signatures of quantum synchronization. New Journal of Physics, 25(2):023012, 2023.

- <sup>37</sup>Wataru Setoyama and Yoshihiko Hasegawa. Lie algebraic quantum phase reduction. Physical Review Letters, 132(9):093602, 2024.
- <sup>38</sup>Arthur T Winfree. Biological rhythms and the behavior of populations of coupled oscillators. Journal of Theoretical Biology, 16(1):15–42, 1967.
- <sup>39</sup>John Guckenheimer. Isochrons and phaseless sets. Journal of Mathematical Biology, 1:259–273, 1975.
- <sup>40</sup>Alexandre Mauroy, Igor Mezić, and Jeff Moehlis. Isostables, isochrons, and Koopman spectrum for the action–angle representation of stable fixed point dynamics. Physica D: Nonlinear Phenomena, 261:19–30, 2013.
- <sup>41</sup>Sho Shirasaka, Wataru Kurebayashi, and Hiroya Nakao. Phase-amplitude reduction of transient dynamics far from attractors for limit-cycling systems. Chaos, 27(2):023119, 2017.
- <sup>42</sup>Alexandre Mauroy, Y Susuki, and I Mezić. Koopman operator in systems and control. Springer, 2020.
- <sup>43</sup>Yoshiki Kuramoto and Hiroya Nakao. On the concept of dynamical reduction: the case of coupled oscillators. Philosophical Transactions of the Royal Society A, 377(2160):20190041, 2019.
- <sup>44</sup>Alexandre Mauroy and Igor Mezić. Global computation of phase-amplitude reduction for limit-cycle dynamics. Chaos: An Interdisciplinary Journal of Nonlinear Science, 28(7):073108, 2018.
- <sup>45</sup>Sho Shirasaka, Wataru Kurebayashi, and Hiroya Nakao. Phase-amplitude reduction of limit cycling systems. In The Koopman Operator in Systems and Control, pages 383–417. Springer, 2020.
- <sup>46</sup>Matthew D Kvalheim and Shai Revzen. Existence and uniqueness of global Koopman eigenfunctions for stable fixed points and periodic orbits. Physica D: Nonlinear Phenomena, 425:132959, 2021.
- <sup>47</sup>Dan Wilson and Jeff Moehlis. Isostable reduction of periodic orbits. Physical Review E, 94(5):052213, 2016.
- <sup>48</sup>Bharat Monga, Dan Wilson, Tim Matchen, and Jeff Moehlis. Phase reduction and phase-based optimal control for biological systems: a tutorial. Biological Cybernetics, 113(1-2):11–46, 2019.
- <sup>49</sup>Peter J Thomas and Benjamin Lindner. Asymptotic phase for stochastic oscillators.

- Physical Review Letters, 113(25):254101, 2014.
- <sup>50</sup>Alberto Pérez-Cervera, Benjamin Lindner, and Peter J Thomas. Isostables for stochastic oscillators. Physical Review Letters, 127(25):254101, 2021.
- <sup>51</sup>Oliver Junge, Jerrold E Marsden, and Igor Mezić. Uncertainty in the dynamics of conservative maps. In 2004 43rd IEEE Conference on Decision and Control (CDC)(IEEE Cat. No. 04CH37601), volume 2, pages 2225–2230. IEEE, 2004.
- <sup>52</sup>Nelida Črnjarić-Žic, Senka Maćešić, and Igor Mezić. Koopman operator spectrum for random dynamical systems. Journal of Nonlinear Science, 30(5):2007–2056, 2020.
- <sup>53</sup>Mathias Thomas Wanner. Robust Approximation of the Stochastic Koopman Operator. University of California, Santa Barbara, 2020.
- <sup>54</sup>Yuzuru Kato, Jinjie Zhu, Wataru Kurebayashi, and Hiroya Nakao. Asymptotic phase and amplitude for classical and semiclassical stochastic oscillators via Koopman operator theory. Mathematics, 9(18):2188, 2021.
- <sup>55</sup>John Guckenheimer and Philip Holmes. Nonlinear oscillations, dynamical systems, and bifurcations of vector fields. Applied Mathematical Sciences, New York: Springer, 1982, 1982.
- <sup>56</sup>Alexandre Mauroy and Igor Mezić. On the use of fourier averages to compute the global isochrons of (quasi) periodic dynamics. Chaos: An Interdisciplinary Journal of Nonlinear Science, 22(3):033112, 2012.
- <sup>57</sup>Crispin Gardiner. Stochastic methods, volume 4. Springer Berlin, 2009.
- <sup>58</sup>Howard J Carmichael. Statistical Methods in Quantum Optics 1, 2. Springer, New York, 2007.
- <sup>59</sup>Crispin W Gardiner. Quantum Noise. Springer, New York, 1991.
- <sup>60</sup>Heinz-Peter Breuer, Francesco Petruccione, et al. The theory of open quantum systems. Oxford University Press on Demand, 2002.
- <sup>61</sup>Daniel A Lidar, Isaac L Chuang, and K Birgitta Whaley. Decoherence-free subspaces for quantum computation. Physical Review Letters, 81(12):2594, 1998.
- <sup>62</sup>Kevin E Cahill and Roy J Glauber. Density operators and quasiprobability distributions. Physical Review, 177(5):1882, 1969.
- <sup>63</sup>John Guckenheimer and Philip Holmes. Nonlinear Oscillations, Dynamical Systems, and Bifurcations of Vector Fields. Springer, 1983.
- <sup>64</sup>Victor V Albert. Lindbladians with multiple steady states: theory and applications. arXiv

- preprint arXiv:1802.00010, 2018.
- <sup>65</sup>Yuzuru Kato and Hiroya Nakao. Quantum coherence resonance. New Journal of Physics, 2021.
- <sup>66</sup>Nikolas Tezak, Nina H Amini, and Hideo Mabuchi. Low-dimensional manifolds for exact representation of open quantum systems. Physical Review A, 96(6):062113, 2017.
- <sup>67</sup>Yuzuru Kato and Hiroya Nakao. Turing instability in quantum activator-inhibitor systems. Scientific Reports, 12(1):15573, 2022.
- <sup>68</sup>Heather A Brooks and Paul C Bressloff. Quasicycles in the stochastic hybrid morris-lecar neural model. Physical Review E, 92(1):012704, 2015.
- <sup>69</sup>JR Johansson, PD Nation, and Franco Nori. Qutip: An open-source python framework for the dynamics of open quantum systems. Computer Physics Communications, 183(8):1760–1772, 2012.
- <sup>70</sup>JR Johansson, PD Nation, and Franco Nori. Qutip 2: A python framework for the dynamics of open quantum systems. Computer Physics Communications, 184:1234–1240, 2013.
- <sup>71</sup>Igor Mezić. Spectral properties of dynamical systems, model reduction and decompositions. Nonlinear Dynamics, 41(1-3):309–325, 2005.
- <sup>72</sup>Stefan Klus, Feliks Nüske, Sebastian Peitz, Jan-Hendrik Niemann, Cecilia Clementi, and Christof Schütte. Data-driven approximation of the Koopman generator: Model reduction, system identification, and control. Physica D: Nonlinear Phenomena, 406:132416, 2020.
- <sup>73</sup>Stephen M Barnett and Stig Stenholm. Spectral decomposition of the Lindblad operator. Journal of Modern Optics, 47(14-15):2869–2882, 2000.
- <sup>74</sup>Hans-Jürgen Briegel and Berthold-Georg Englert. Quantum optical master equations: The use of damping bases. Physical Review A, 47(4):3311, 1993.